

NO. 36. RADIAL STRUCTURES SURROUNDING LUNAR BASINS, II: ORIENTALE AND OTHER SYSTEMS; CONCLUSIONS

by WILLIAM K. HARTMANN

June 20, 1964

ABSTRACT

A new analysis of mare basins begun by Hartmann (1963) is concluded with this paper. The radial systems of the oldest basins are the least developed, while those of the young basins — Mare Imbrium and Mare Orientale — are the most prominent. It is therefore hypothesized that conditions for producing radial lineaments were optimum during the relatively short period when the mare basins were flooded. Many lineaments are spatially associated with this flooding. The basins are probably the sites of great impacts which were accompanied by radiating fractures. Most lineaments are interpreted as the expressions of tectonic adjustments in the stressed crust along these fractures as a result of heating of the subsurface. Most of the adjustment appears to be by vertical motion. There is little evidence for horizontal motion or for gouging of radial valleys by flying fragments. The discussion includes reviews of the nonradial grid patterns and of the small radial systems around some recent craters.

1. Introduction

This paper completes a new and independent study of radial basin systems, founded largely upon rectified photography. The Imbrium system was surveyed in Part I (*LPL Comm.* No. 24, 1963). In Part II the discussion is extended to other basin systems and further suggestions are offered as to their significance. Astronautical directions are used, as before. For each basin, the surroundings are described under subheading (a) and interpretations under (b).

2. The Orientale System

(a) Morphology

Plates 36.1 through 36.6 show the Orientale System radial structures. With the sunrise terminator near longitude 80° W (good sunset pictures are lacking at the narrow crescent phase), a major family of linear features is seen NW of Wargentín. This aspect is shown in Plate 36.1. Rectified photography at once reveals the convergence of the linear features. Plate 36.6a, centered over Orientale, reveals

the concentric scarp system and confirms that the convergence is toward the Orientale inner basin. It is clear that the Orientale basin, second only to the Imbrium basin in the magnitude of its concentric ring system (Hartmann and Kuiper, 1962), is also second only to Imbrium in the prominence and extent of its radial system. Plates 36.1 and 36.2, taken with low lighting, demonstrate the great extent of the Orientale radial family toward Wargentín.

Comparison of Plates 36.2 (low lighting) and 36.3 (high lighting) shows, as did 24.14 and 24.18 for the Imbrium system, that there is no prominent ray system radial to Orientale, and that the radial system is structural, not surficial. Plate 36.3 also reveals the small mare at the center of the basin system.

No radial structure is found inside the Eichstadt ring. Outside this ring, running to the SE, are several shallow valleys, some 30 km across. These valleys merge to the S with arcs of the SE limb basin system (Hartmann and Kuiper, 1962, p. 57, Pl. 12.45). In this same region, and out as far as Inghirami, the

mountainous uplands have a pronounced radial and concentric, nearly orthogonal, pattern. Some of the radial structures, such as those running toward the NE rim of Inghirami (best shown in Pls. 36.1 and 36.2) are clearly neither narrow valleys nor mountain ridges, but scarps, probably bounding broad depressions. The whole region gives the impression of a crustal mass fractured along nearly orthogonal lines.

Further out, beyond Inghirami and near Bailly, are curious structures formed by 10–20 km craters with narrow valleys running SE out of them away from Orientale. They can be seen clearly in Plate 36.2, and some may be seen under the very low lighting and high resolution of Plate 36.4. The valleys are on the order of 10 km across and have slightly-raised rims (see Pl. 36.4). On the floor of Schickard may be seen some further examples which appear to be buried by the mare material in that crater.

To the E and NE of the Orientale basin the radial structure is not nearly so pronounced. None is prominent in the region due east of Mare Orientale (see Pls. 36.5, 12.32–12.34). In Plate 36.5, showing the northeastern regions from above Grimaldi, we find such structures just outside the Eichstadt ring. It is remarkable that so many of these lineaments show in spite of being oriented nearly perpendicular to the terminator. Here again in the rough uplands is distinguishable a nearly-orthogonal pattern symmetric with Orientale. Locally, e.g., NE of Schlüter, the pattern resembles a Cartesian grid rather than a radial fan, though the relationship to Orientale is clear from the grid orientation.

Just ENE of Schlüter there occurs a pair of striking grooves, typical of radial structure, but not aligned with Orientale. These and several other lineaments are much more closely aligned with Imbrium (see Pl. 36.6 *b*) and may be outlying members of that system. All prominent lineaments in the regions so far considered appear to be attributable to either Orientale or Imbrium.

The radial structure of the Orientale basin system is summarized in an overlay on Plate 36.6*b*. Comparison of the Orientale system with the Imbrium system shows the Orientale radial structures to be profuse as far as 48° selenocentric SSE of the basin, while the comparable figure for the Imbrium system is at least 80° selenocentric. Thus the ratio of the sizes of the radial systems is roughly 0.6. The Orientale structure begins just outside the Eichstadt ring, which is therefore analogous to Imbrium's

Apennine ring. The ratio of diameters of these rings is roughly 0.7. We may therefore consider the Orientale radial and concentric system to be two-thirds the size of the Imbrium system.

Imbrium is flooded up to and beyond its Apennine ring (diameter 1340 km); Orientale is flooded only inside its innermost ring (diameter 320 km) and in arcuate patches along the base of the Eichstadt ring and its inner companion.

There are also differences in the forms of the major radial structures. The well-known Imbrium gashes, characteristic of the Ptolemaeus region, are rare in the Orientale system. The valleys near Schickard (Pl. 36.4) are their closest analogue. The Imbrium structures, which in Part I were associated with *flooding*, e.g., broken crater walls, split mountain masses, mountain ridges, etc., are absent here. On the other hand, the local orthogonal patterns present in Orientale are not so characteristic of Imbrium.

The Orientale system shows more asymmetry in azimuth than does the Imbrium system. It has often been stated that the Imbrium radial system is highly asymmetric, being concentrated in the sector from the Haemus Mountains to Ptolemaeus. However, it must be noted that this is the only well-observed region of old upland surface close to Imbrium and that radial systems are well seen only on such a surface. Other upland regions around Imbrium are either small or near the N limb. Plate 24.40 shows that some radial structure is found on uplands in all directions from Imbrium, although the greatest density is indeed in the Ptolemaeus direction. The Imbrium radial system is thus only slightly asymmetric. In the case of Orientale, on the other hand, the basin is bordered by uplands on *all* visible sides, and it is clear that the radial structure is asymmetric and highly concentrated toward the SE.

In interpreting these photographs one must bear in mind the distortions inherent in rectification. In any depression near the W limb, the W inner wall is seen, but the E inner wall is mostly hidden; thus the rectified photographs cannot reveal the whole interior.

(*b*) Interpretation

The Orientale radial and concentric system is second in magnitude only to that of the Imbrium basin, but it shows significant differences in appearance. If the various lunar basins were caused similarly, the question arises how one can account for these differences. The most promising hypothesis is

that they were formed during different stages of lunar evolution. Evidence was summarized in Part I that the Imbrium event occurred near a period of maximum surface heating, when the crust was already subject to subsidence into softer subsurface layers, and when the dark mare material had its maximum accessibility to the surface. Hartmann and Kuiper (1962) pointed out that the Orientale basin is a relatively recent feature. Its ring system has a fresh appearance. Its radial system is superimposed on the SE limb basin, and cuts the floors of Schickard and Bailly. The distribution of mare material is explained if the subsurface was already cooling and material could reach the surface from depth only in the highly-disturbed center and along concentric scarps. For these various reasons the Orientale basin is supposed to have originated *late* in the period of mare formation.

The orthogonal appearance of the unflooded uplands toward Inghirami appears to be due to block faulting. It is a different pattern from the orthogonality noted in parts of the Imbrium system, which was related to modification during flooding. It does not seem possible to explain either this orthogonality or the structural differences with Imbrium under the hypothesis of sculpture by projectiles from a central explosion. The hypothesis of tectonic activity allows a greater range in structures. If the late-mare crust of the Orientale region were less plastic than the late pre-mare crust near the Imbrium impact, the Orientale system would show more of a shatter pattern than the Imbrium system, as it actually does.

The craters with trailing valleys (shown in Plates 36.2 and 36.4), farther away from Mare Orientale, may be impact sites of flying fragments. They are similar to some very small Imbrium valleys, shown on USAF-NASA chart LAC-77 (1963). The discussion in Part I (p. 7) shows that the larger Imbrium radial valleys tend to have craterform segments, but not preferentially at one end. An example of nonimpact craters at the ends of rille-like valleys is seen NE of Aristarchus in Plate 36.23*d*.

We have seen that the Orientale radial system is highly asymmetric in azimuth. This phenomenon has been attributed to nonisotropic stresses from a non-vertical impact (Urey, 1961). In this case the crust may have been compressed and broken to the SE when a large body impacted in the present inner ring from the NW at a low angle. Why, however, is the concentric ring system so much more isotropic than the radial system? Possibly, the concentric ring system is due primarily to the isotropic shock waves

from a central explosion, while the radial structures are caused primarily by the horizontal component of the momentum imparted to the crust by the impacting body. Hartmann and Kuiper (1962, pp. 62–63) consider both (1) faulting along concentric fractures which were caused by the impact, and (2) crustal compression from horizontal momentum components as possible causes of concentric arcs. Alternative suggestions are Baldwin's (1963, p. 317), that the arcs are frozen shock waves; and Fielder's (1963*a*), that basin systems are internally produced through faulting and not related to impacts.

3. The Nectaris System

(a) Morphology

Plates 36.7 through 36.12 show regions near Mare Nectaris. Plate 36.12, centered over Nectaris, is best for an overall view of the system.

In the arc from S to NW of the Nectaris basin lies an expanse of upland where one would expect to find radial structures analogous to those of the Imbrium and Orientale systems. However, no prominent Nectaris radial system is found there in spite of the fact that the concentric system finds its most prominent expression — the Altai scarp — in this direction. R. G. Strom (1964) has pointed out some minor lineaments SW and NW of the basin, which are part of a more general global pattern.

Also, as might be expected from the Imbrium discussion, there are no radial structures on the mare surfaces NW to NE of Nectaris. The small upland area near Capella and Isidorus, N of Nectaris, shows few prominent Nectaris radial structures. The single prominent valley cuts through Capella and is nearly aligned with Imbrium (see Pl. 12.3).

In the arc from E to S of the Nectaris basin is found a whole family of linear valleys. The three most prominent of these are the Rheita Valley (defined in the IAU catalogue of Blagg and Müller, 1935, to extend from near Rheita to Young); the narrow valley extending S from Young through Mallet, called here the Mallet Valley (sometimes incorrectly taken to be a part of the Rheita Valley); and the long valley running through Snellius, called here the Snellius Valley (see Pl. 36.12). In the following paragraphs, some characteristics of these three are enumerated.

(1) The approximate dimensions are: Rheita Valley, 25 by 330 km; Mallet Valley, 12 by 190 km; Snellius Valley, 23 by 800 km.

(2) Each of these valleys is broken by relatively recent craters (e.g., Rheita), but each disturbs older craters (e.g., Young, whose walls and floor are broken).

(3) The two larger valleys (Rheita and Snellius) exhibit craterform segments. In the Rheita Valley these are separated by parallel transverse ridges, and the segments so defined do not resemble the normal craterlets of the surrounding uplands. The Snellius Valley most clearly shows craterform segments and its western part strongly resembles a crater chain.

(4) The three valleys have rims which are very slightly raised relative to the surroundings (e.g., see Pls. 36.7, 36.10a, and 36.11).

(5) The interior of the Rheita Valley displays considerable detail in the form of minor ridges and valleys (in addition to the transverse ridges) and the Snellius Valley is even more broken. The Mallet Valley appears to be more regular.

(6) The Mallet Valley departs by about 12° from the direction of the Rheita Valley. Because of this and the differences in form, it should not be assumed that these form a single structural unit.

(7) The Snellius Valley displays an *en échelon* pattern, especially clear at its E end (see Pl. 36.10).

(8) The Mallet Valley is quite accurately radial to the Nectaris inner basin, but the Rheita Valley is nearly tangential to it. The Snellius Valley's *en échelon* pattern defines a parallel family whose central member is approximately radial to the Nectaris inner basin.

In addition to these major valleys there are a great number of smaller valleys, especially near the Rheita Valley, E of Janssen. This area is well shown on the matching Plates 36.8 and 36.9 (sunrise and sunset views, respectively). The valleys converge approximately toward the center of the Nectaris basin. Of the three larger valleys discussed above, they most nearly resemble the Mallet Valley. They do not exhibit such clear craterform segments as the Rheita and Snellius Valleys. They do have slightly raised rims. They are close to the limb and difficult to interpret adequately, but bear some resemblance to the Imbrium valleys near Ptolemaeus.

A pair of linear scarps runs from Janssen toward the Nectaris inner basin. They are well seen on Plates 36.8 and 36.9. The E side of each scarp is the higher. The eastern scarp is about 300 km long; the western, at least 120 km. The N end of the eastern scarp terminates abruptly where it touches the Altai ring just E of Piccolomini. In its central parts can be seen

a resemblance to a valley with craterform segments. Both scarp directions are nearly tangent to the inner basin (see Pl. 36.9).

All of the structures discussed so far lie outside the outer ring of the Nectaris basin system. The only prominent radial pattern to be found within the Altai ring is best shown in Plate 36.7, where a radial trend can be detected in the mountain masses in the arc from S to E of the inner basin. This trend continues outside the Altai ring and it is in this same direction that the major valleys are found still further out.

The system of valleys and scarps described above is identified here as a Nectaris system because most of the structures converge toward the Nectaris inner basin. Gilbert (1893) and others have attributed the major valleys to the Imbrium system. Plate 36.12, centered over Nectaris, also shows part of Imbrium's Apennine arc, and one sees that the valley system is more nearly symmetric to Nectaris. Nonetheless, the region is marked by many outlying members of the Imbrium system.

The degree of convergence of the Nectaris system is not as great as in the Imbrium or Orientale systems, but the rule still applies that the trends of the structures pass within or are tangent to the inner ring of the basin system. This system, with its many valleys, resembles the Imbrium system more closely than it does the Orientale system; yet it is analogous to the Orientale system in its nonuniform distribution in azimuth.

Comparing the extent of Nectaris and Imbrium systems, we find that the Nectaris radial system can be traced as far as 42° selenocentric from the basin center, 53% of the comparable distance in Imbrium. The structures begin at the Altai ring, which has a radius 63% of that of the comparable Apennine ring of Imbrium. Similarly, the ratio of inner basin diameters is 0.60. The scale of the Nectaris basin system is thus about 0.6 that of the Imbrium system.

(b) Interpretation

Although the features discussed do not all show precise convergence toward the center of the Nectaris inner basin, they do define a pattern associated with Nectaris.

The Nectaris radial system appears to be of an intermediate pre-mare age, based on the observation that the system cuts and is cut by many craters. Because of the large number of superimposed craters we conclude that the Nectaris radial system is older than the Imbrium and Orientale systems. The same is true of the concentric system. These results agree

with independently assigned ages based on pre-mare crater densities in the systems, as described by Hartmann and Kuiper (1962, pp. 52–53).

Regarding the formation of the valleys, we may rule out a simple splitting-apart of the crust, suggested for the Alpine Valley of the Imbrium system (see the review of literature in Hartmann, 1963, pp. 2, 4). This hypothesis would not account for (1) the circular outline of Young (not deformed though the Rheita Valley cuts its floor and walls), (2) the transverse ridges, (3) the slightly-raised rims, and (4) craterform segments within these valleys. Apparently there have been no horizontal shifts in forming the valleys.

Gouging by flying fragments does not satisfactorily explain (1) the transverse ridges, and (2) the craterform segments. Fielder (1961, p. 184) also lists arguments against an external origin.

Some sort of tectonic activity and subsidence along major faults accords with the observations. The observed *en échelon* pattern of the Snellius Valley is a known characteristic of terrestrial fault structures. DeSitter (1956, p. 157) states that "normal faulting often shows an *en échelon* arrangement" and that among wrench faults (p. 174), "an *en échelon* arrangement is not common, but in general the wrench-faults are accompanied by many smaller parallel faults of the same character." Although subsidence *alone* does not account for the raised rims, subsidence does appear involved. The craterform segments do not conflict with this interpretation, for evidence was cited in Part I, p. 7 relating crater chains with graben-like features. Furthermore, other authors (e.g., Shoemaker, 1962, pp. 298–303; Rittmann, 1962, pp. 88–92; and Fielder, 1961, pp. 210–216) have discussed the development of lunar and terrestrial craters and graben along deep-seated faults. The two scarps N of Janssen may mark faults along which full-fledged valleys never developed.

Because even the terrestrial examples are not completely understood, it is not profitable to try to describe in further detail the processes which occurred along the hypothetical deep-seated lunar faults.

There are fundamental differences in form among the various rilles, crater chains, graben, and radial valleys of the lunar lineaments. The writer suggests that these are due in part to differences in depth of the underlying faults and in the accessibility of magma and gas to the surface. These differences may in turn be due to the different epochs during

which the particular basin systems formed, as suggested above. The evidence already cited that the Nectaris system formed before Imbrium and Orientale would thus be in accord with the differences in form of these systems.

Nectaris shows evidence that the development of the radial and concentric systems occupied an extended period of time. The inner basin itself is old and pre-mare, as evidenced by the many superimposed, post-basin, pre-mare craters; and the radial valleys appear to be pre-mare on similar grounds. However, the Altai scarp must have formed later and may even be post-mare, judging by its fresher appearance and the relative lack of major craters along its length. Such a difference in appearance (and presumably age) within a single ring system is inconsistent with Baldwin's (1963, p. 317) interpretation that the concentric rings are frozen shock waves.

4. The Humorum System

(a) Morphology

Plates 36.13 through 36.16 show the region of Mare Humorum. As expected, no radial pattern is visible in the maria N and E of the Humorum basin, although Plate 36.16 shows lineaments in the Rhiphaeus Mountains in neighboring peaks.

SE of the basin, as shown in Plate 36.13, aligned ridges are found. Study of the plate reveals a family of parallel structures, most prominent near the center, and on a line radial to Humorum. There is a resemblance to the Imbrium system in the sense that many of the ridges in this partly-flooded region mark portions of older damaged craters.

The same description applies S of the basin. The parallelism here is aligned in a different direction from that of Plate 36.13, but again it is most prominent near the line radial to the basin.

SW of the basin is found a very striking orthogonal pattern of ridges and broken-down craters. This is shown in matching Plates 36.14 and 36.15 (morning and evening, respectively). Most of the structural lines are associated with old craters which have been modified, and there is some localized flooding (cf. Pl. 36.3). In these respects the region is similar to the Haemus Mountains in the Imbrium system (cf. the square crater Auwers, Pls. 24.6 and 24.7, and portions of the Orientale system, Pl. 36.5). This part of the Humorum lineament system is parallel, not radial. The width of the region of local parallelism is roughly equal to the diameter of the inner

basin and in the center of the region the direction is radial to the basin. There are two predominant directions of trend, NE-SW and NW-SE. The line of symmetry is directed to the center of Mare Humorum.

(b) *Interpretation*

The Humorum basin is accompanied by several families of nearly-parallel lineaments; the members of each family are strongest where the direction is strictly radial. Together, these families define a radial system and therefore are related to the basin. The structures of this radial system exhibit both differences and similarities to structures of previously discussed systems. The Humorum system exhibits no major valleys but, rather, a system of ridges and oriented crater-wall remnants in regions of local flooding. The Nectaris system, on the other hand, consists primarily of valleys. Imbrium shows both types of structure. The most prominent feature of the Orientale radial system is a pattern of nearly-orthogonal faults, whereas flooding is very limited and with it, the process of crater destruction.

We have already suggested that these differences reflect varying ages of the basins. The observations of the Humorum basin suggest this structure is of intermediate pre-mare age. In view of the fact that the major valley systems of Imbrium and Nectaris occur in the unflooded uplands while the ridge systems of Imbrium and Humorum occur in partially-flooded regions, it appears that the nature of the radial structure is correlated with the degree of local flooding.

Fielder's recent study (1963) of the grid system includes a discussion of Humorum. He lists a number of structures in the Humorum system which must have been *internally* produced, including faults along the mare edge, concentric rilles, and wrinkle ridges. In this respect Fielder and the writer are in close accord: the evidence indicates extensive tectonic activity. But he continues (p. 83),

"All these features are characteristic of the rudely circular type of lunar mare. The conclusion that Mare Humorum is a sink, like Mare Imbrium, is inescapable."

"... other maria — in particular, Mare Nectaris, which is also obviously an igneous sink — might have been chosen to illustrate many of these points."

Fielder's argument apparently is that if many structures intimately associated with a basin are internally produced, then the basin itself must have been internally produced. The writer has endeavored to show in Part I and here that, on the contrary, the coupling of the impact hypothesis of basin forma-

tion with the hypothesis of extensive tectonic activity allows explanation of the various observed features. It provides for the radial fractures along which activity occurs; it also explains the varying time lags between basin formation and mare formation, which are not predicted by the sink hypothesis.

5. *The Crisium System*

(a) *Morphology*

Near the Crisium basin, shown in Plates 36.17–36.19, there are very clear examples of lineaments forming orthogonal patterns. A plot of these reveals symmetry with the basin, as seen in Plate 36.19. Reference is made to Fields 14 and 15 in the *Rectified Lunar Atlas* (Whitaker, *et. al.* 1963) for further illustrations.

The clearest examples are found NW of the basin, toward Posidonius. In the depressed, partly-flooded zone, between the inner ring and the outer scarps, are ridges and rectilinear outlines of flooded depressions (see Pl. 36.17). The lineaments are more nearly parallel than radial, but the pattern is strongest where the common direction is radial to the basin, as was found with other basins. There is a remarkable resemblance between this area and the rectilinear structures of the depressed, partly-flooded zone of the Imbrium system just inside the Apennine ring (see Pls. 12.26 and 12.27, and bottoms of Pls. 24.8–24.10).

The same rectilinear pattern can be traced on other sides of the basin, particularly on the SW, where one of its directions is again radial. This is seen in Plate 36.18 where the SW arc of the basin wall consists of a step-like pattern of lineaments. The overlay of Plate 36.19 maps the pattern, showing its presence also in the NE.

Additional lineaments can be seen in Plates 36.18 through 36.19. Many flooded depressions to the SE are bounded by straight sides radial to the Crisium center, and other linear structures can be found in the uplands by careful study of various photographs, not all reproduced here. They are mapped in Plate 36.19. Near the limb, the interpretation of structure is difficult, but ridges and scarps appear to be the most common.

More than any other basin, Crisium exhibits local parallelism of lineaments. West of Crisium the predominant lineaments are not radial but continue the orthogonal pattern which is more clearly seen in the NW and SW. The Crisium basin resembles the Humorum basin in the degree of local flooding, in

the parallelism of nearby lineaments, and in the absence of major valleys.

(b) *Interpretation*

As with the basins discussed above, it is concluded that the lineament pattern near the Crisium basin is causally related to it. Fielder, examining the grid system (1961, p. 177) states that

"... careful examinations reveal that [near both Mare Humorum and Mare Crisium] these localized ridges and valleys are specially placed components of a more general family of parallel striations. Clearly, some components of any family of parallel lines which intersect a circle will run along radii of the circle, and it would seem that the two cases cited would be examples of this situation."

The present study shows that there are prominent lineament systems genetically related to neighboring basins; these are not chance juxtapositions of a global grid system and the circular basins. The supporting evidence may be summarized as follows: (1) the indisputable presence of accurately-radial systems around several major basins, e.g., Imbrium and Orientale; (2) the greater prominence of parallel families where the direction of parallelism coincides with the radial direction; (3) the close resemblance in "fine structure" of some of the members of the Crisium and Humorum families with members of the Imbrium system (cf. Plate 36.25, below); (4) the presence of local parallelism within the radial systems of craters like Aristillus (see Sec. 8).

Yet the continuity of the orthogonal pattern, even in places where it is not radially symmetric with a basin, is evidence for the existence of a more widespread grid system, especially in the vicinity of the Crisium basin. Other influences, such as crustal stresses, must have caused such a wider grid system. Lines on Plate 36.19 indicate the directions to the center of the Imbrium basin system. The lineaments under review do not follow the Imbrium direction.

All of these facts are consistent with the concepts that (1) the radial systems are the expressions of fractures created at the times of formation of the basins; (2) the basins are of different ages, mostly pre-mare; (3) the fractures of the grid pattern were superimposed on the radial fractures; and (4) virtually all of the visible lineament structure evolved along these fractures before and during the period of mare formation.

6. *Other Basins*

The Mare Humboldtianum basin is seen in Plates 36.20 and 36.21. Accurately radial to the

inner basin, and extending roughly 140 km between the inner and outer scarps toward the SW, is an unusually straight scarp, revealed by its shadow on Plate 36.21. Comparison of the opposite-lighting views of 36.20a and 36.21 indicates a row of hills on this line, with the scarp facing SE. Plate 36.20b shows patchy flooding along the lineament. Our interpretation is that we see a fault scarp with lava extruded along its base. This interpretation was also given to the Orientale scarps along which one finds flooding (Hartmann and Kuiper, 1962, p. 57).

Between Humboldtianum and Crisium are several linear features, well shown in Plates 36.20a and 36.21. The clearest example is a scarp facing E, curiously smoothed, not sharp, as is the Straight Wall. It might be termed a "ghost scarp." Its surroundings are smooth but bright, neither rugged upland nor mare. Other minor structures, mostly scarps and ridges, in an area of partial flooding SW of Humboldtianum, appear to form a radial pattern. However, identification and interpretation is difficult so close to the limb.

Grimaldi, Janssen, and a basin near Schiller are remaining multi-ring systems discussed in *Communications* No. 12. None of these shows clear radial structure. Judging by subsequent damage, we conclude they are early pre-mare structures.

Other mare basins which give little or no evidence of radial structure include Serenitatis, Nubium, Smythii, Marginus, and the basin on the limb NW of Bailly. Significantly, none but the latter shows well-defined concentric structure. All of these give the impression of being relatively old basins, judging by sharpness of the walls and extent of subsequent damage. The term basin is applied because of the size of the circular bounding walls, which can only be partially traced in most cases.

It is seen that as one proceeds from the youngest basins, dating from the mare epoch, back through the older pre-mare basins, the radial systems become harder to trace, and generally become subordinate to weak local grid patterns. To a lesser extent, the concentric scarps also become harder to trace but they are less clearly related to the local grid directions. Similar observations apply as one proceeds from larger basins through smaller basins to crater-sized objects.

Figure 1 summarizes the observations of all of the radial systems discussed so far, based on an unrectified full-moon photo. The Imbrium system shown here is based on Plate 24.40 in Part I. Some lineament patterns not clearly related to basin sys-

tems are shown by dotted lines. They were noted during the preparation of this paper, but no attempt was made to map all of them.

7. Grid Systems

The term "grid" was apparently first applied by Spurr (1948), who used it to refer to a global system of fractures. Spurr spoke primarily of a polar-grid fracture system, most prominent near the poles, and with nearly-meridional members. He suggested symmetry with respect to the moon's equator and central meridian. Spurr (1948, p. 101) proposed that the polar grids were older than the Imbrium system and that they arose when the moon's rotation became synchronous with its revolution.

The concept of a grid system defined by lineaments has aroused wide interest in the past 15 years. Fielder (1961, pp. 180–195) gives an excellent review of the work done, and reproduces charts by various authors. He includes the polygonal shape of some craters as part of the grid concept, and traces such discussions back more than 50 years (Fielder 1961, p. 180).

There is some ambiguity in the use of the term "grid system." Virtually every author who recognizes the validity of the term considers the systems to be tectonic, internally-produced phenomena. Further, it is usually implied that local grid patterns can be combined into one global system which had its origin in a global phenomenon such as a change in rotation rate, shift in polar position, contraction, or expansion. Nevertheless, all of the grid system charts reproduced by Fielder (1961) include the Imbrium radial system, which is definitely a local system. The present paper shows that systems of lineaments accompany other major basins as well. Therefore, if "grid system" is to refer to a single global pattern only, the local radial systems should be excluded, except insofar as they show systematic asymmetries.

Baldwin (1963, p. 385) makes the additional criticism that merely mapping linear formation is not sufficient for grid-system analysis because the resulting charts will mix old and young features of different types, such as wrinkle ridges, valleys, and sections of crater walls. This mixing has in fact occurred as can be seen from the charts reproduced by Fielder.

The following additional points are made regarding the grid systems:

(a) The writer defines as a *grid system any background pattern of lineaments not clearly related to any individual basin*. Therefore, symmetric radial

systems must be subtracted before a study of a grid system is made, although asymmetry in density or direction of radial structures may be related to grid systems. In fact, there *appears to be a preference for radial structures extending SE from basin centers*. In these radial systems there is a tendency to favor SE-NW strikes, and to a lesser extent SW-NE strikes, producing a pattern not unlike that predicted by Vening Meinesz (1947) to result from a change in the planetary rotation axis. This diagonal preference around basins is probably related to the diagonal global network noted by Fielder (1963, pp. 72–75).

(b) The lineaments defining the grid systems are, for the most part, less prominent than those in radial systems.

(c) Evidence has been found for *localized manifestations of grid systems*. We have already seen that in the older basins, the radial pattern is characterized by families of locally-parallel lineaments. The identity of these families is maintained even where their dominant direction is nonradial. Second, there are lineament families not radial to any nearby basins. An example is the well-known lattice pattern near Arzachel, mapped in Plates 24.20 and 24.21 of Part I. This system appears to be very old. Neither Nubium, Serenitatis, Tranquillitatis, nor Nectaris is in a symmetric position to this pattern, and it does not increase in prominence toward any of them. A more unusual example is the well-defined lineament pattern which includes the Ariadaeus Rille, the parallel branch of the Hyginus Rille, and an *en échelon* extension of the Hyginus Rille westward. This family differs from most in being quite young.

(d) The local grids consist of structures similar to those forming the radial systems. Both classes of structure probably have tectonic origins.

(e) In addition to local grid systems, there is evidence for one or more global grid systems. These are not discussed here but are being studied by R. G. Strom (1964) of this Laboratory.

8. Radial Systems Around Craters

Many craters display radial patterns. This is best seen around young craters on the nearly featureless mare surfaces. Here, one observes a coarse radial pattern in the hummocky raised rim, grading into a pattern of fine ridges and valleys, from a few kilometers width on down, on the surrounding mare. It is well known that these systems exhibit a local parallelism similar to that described here in the radial systems of basins (See Warner, 1961, pp.



Fig. 1. Schematic diagram of lunar basin systems. Each line marks a concentric or relatively prominent radial lineament and each is drawn to proper scale and orientation. Dotted lines give examples of some prominent local grid patterns, not related to basin systems.

391–392). Some examples are shown in Plates 36.22 and 36.23.

Baldwin (1949, p. 208), proposing that the sequence from small crater pits to the large mare basins represents only a size range in a single family of impact structures, described the radial systems of craters simply as reduced versions of the basin radial systems. The writer regards this description as valid only in a limited sense for the reasons which follow.

The coarse radial structures in the rough rims of these fresh craters indeed resemble the coarse pattern observed in the Apennine rim of Imbrium and perhaps in the rim of the Orientale basin. We have already identified these basins as relatively recent, and commented on the lack of flooding in the Apennines and Orientale region. Therefore, this type of radial structure can be regarded as the immediate and unaltered result of buckling of the crust on impact and emplacement of debris on the outer rim. Its presence in both well-preserved craters and basins supports Baldwin's conclusion that craters and basins are of similar origin.

However, the many other radial structures in large basin systems, e.g., pre-existing mountainous areas broken into ridges, damaged craters, and troughlike structures, find no counterpart in the radial systems of fresh craters. Yet this is in accord with the ideas here presented, as these structures have been attributed to tectonic processes along fractures and related to the high-temperature mare epoch. The craters recent enough to be well preserved are post-mare. Furthermore, it is likely that crater-sized objects are too small to provide suitable conditions for the development of tectonic radial structure.

The most delicate lineaments, e.g., those which radiate at least 160 km from the center of Aristillus, have no known counterparts in the basin systems because they would lie in the rugged uplands where their fineness would prevent detection. Available photos lack sufficient resolution to prove whether these ripples represent fracturing or buckling of the crust, or grooving by fragments blown out by impact. D. W. G. Arthur (private communication, 1963) favors the latter view on the basis of high-resolution visual studies.

There remain important differences between craters and basins. The preference of the mare material for the large basins is easily explained if this material is lava. Because of greater damage to the lunar crust at the largest impact sites, lava had

easier access to the surface. The most puzzling difference is the presence of the concentric rings around the basins, with no trace of them around either the recent craters with radial structures, or around some pre-mare craters of basin dimensions. To explain this, one may have to appeal to differences in impact velocity or possible differences in the impacted crust.

9. Conclusions and Summary

The primary result of this paper is the conclusion that a system of radially-oriented lineaments is an integral part of the typical mare basin system. The radial structure can be traced, in some cases, as far as seven times the radius of the innermost ring of the concentric ring systems of these basins. This concept of a basin system with radial and concentric structure has been heavily influenced by study of the best-preserved and largest examples, Imbrium and Orientale.

The basins are of varying ages, but the mare surfaces stem more nearly from one epoch. This has been well documented by Baldwin (1949, pp. 211–212; 1963, pp. 304–309), Shoemaker, Hackman, and Eggleton (1962, Table 2), and Hartmann and Kuiper (1962, pp. 62, 65). The basins can be placed in an age sequence by consideration of: (a) sharpness of concentric walls, (b) density of post-basin, pre-mare craters, and (c) extent of flooding. When the basins are considered in this sequence, it is found that with increasing age the radial systems become less well defined. The basins are tentatively classed by increasing age as follows: Orientale, late-mare; Imbrium, late pre-mare or early-mare; Humboldtianum, Nectaris, Crisium, Humorum, Serenitatis and the smaller basins, pre-mare.

Numerous observations of special interest have resulted from this survey of the radial systems:

(a) No known radial system is post-mare. A few scattered individual features such as the Straight Wall and Cauchy scarp are probably post-mare.

(b) The bulk of the structures cannot be accounted for by the grooving action of flying fragments. Most of the structures form nearly-orthogonal patterns of ridges and depressed, often-flooded zones. Major valleys, which have been considered the prime evidence for grooving, are confined mostly to the upland parts of the Imbrium and Nectaris systems. Their characteristics — craterform segments, transverse ridges and other structures on their floors, darkness of their floors, *en échelon* patterns (e.g., Snellius

Valley), etc. — indicate that not even they originated by grooving.

(c) No horizontal motion has been found in the study of the radial systems (cf. also Baldwin, 1963, p. 375, and others) and the Rheita Valley shows definite evidence against horizontal displacement. Vertical motion must dominate. This finding differs from Fielder's (1963, p. 87) conclusion from a study of the grid system that "strike-slip faults are of even greater importance on the moon than are normal faults."

(d) The *en échelon* pattern of the Snellius Valley strongly suggests faulting.

(e) Repeated evidence is found in various localized regions that the structures of the crust have been modified in some cases to the extent of complete destruction (see also Hartmann, 1963, p. 10). Best evidence for this is found among structures of the Imbrium and Crisium systems. Near mare surfaces there is often a clear association of this phenomenon with the mare material, but examples can also be found in unflooded upland regions.

(f) Some radial systems show an asymmetric distribution in azimuth, even after allowance for disappearance by flooding. This is most clearly seen in the uplands around Orientale and Nectaris. It is not so definitely known in the case of Imbrium, because of the extent of flooding, but there is probably a concentration toward the SE. In both Orientale and Nectaris, the concentric system is more uniform in azimuth than the radial system.

(g) In the typical basin system, most of the radial structure lies beyond the outermost concentric ring. The pattern found within the concentric ring system is usually limited to flooded regions of subsidence.

(h) A certain unity exists among the different radial systems, as may be seen by noting the similarity of radial lineaments in different parts of the moon. Plates 36.24 and 36.25 give such a comparison at uniform scale. In plate 36.24, valleys from widely separated points on the moon are compared. Plate 36.25 gives 3 examples each of (1) flooded regions showing orthogonality, (2) scarps, and (3) craters broken into linear segments. The form of the predominant lineaments may nonetheless vary from one basin system to another.

(i) Independent of the radial systems, there exist patterns of lineaments which define local "grid systems." Study of these is beyond the scope of this paper. A consideration of grid systems as a global phenomenon must take into account the presence

of independent radial systems around basins.

Having listed the chief observations, we now attempt to fit them systematically into a hypothesis of the development of the lunar surface. On the basis of telescopic observations alone, one is led to the conviction that there was a period of extensive tectonic activity during which many pre-existing structures were damaged and the mare material was deposited. Reference to theoretical work of the last decade suggests that this was the period of maximum radioactive heating at the surface. This period conveniently divides lunar history and is called here the *mare epoch*. The following model is believed consistent with all of the observed facts.

In the pre-mare period most of the craters formed. The basins either are unusually large examples of these ordinary craters, or represent a separate class of objects. In support of the first interpretation, the distribution of crater diameters D with respect to number of craters n is given by $n = cD^{-2.1}$ where c is a constant (Hartmann, 1964). Thus, the basins may represent one extreme of this distribution. It should be possible to check this quantitatively when a larger sample of craters has been measured. In support of the latter interpretation are the differences in form between basins (with their concentric and radial patterns) and ordinary craters. Both craters and basins are probably impact features. As each basin formed, it probably acquired some radial structure around its walls, analogous to that seen in recent crater rims. But, just as importantly, many radiating fractures were formed. The direction and velocity of fall, and the presence of any pre-existing stresses in the surface were probably important factors in determining the distribution of these fractures. The nature of the surface, the presence of local stresses, the time interval from basin formation to maximum heating, and the degree of local heating were probably important factors in the development of tectonic adjustments along these fractures.

These developments must have occurred throughout the interval between basin formation and the close of the mare epoch, in view of the following observations: (a) coarse radial patterns are thought to be original features of the basin rims; (b) some structures appear to be pre-mare (e.g., valleys in the Nectaris system); (c) other structures in the same systems appear to be younger than those under (b) (e.g., Altai scarp); (d) even in older basin systems, there is a correlation between the degree of local flooding and the presence of certain types of radial structure (e.g., partially destroyed craters in Im-

brium and Humorum systems), suggesting that these particular structures formed during the mare epoch; (e) the mare surfaces are virtually never broken by post-mare radial structure.

We have noted that radial systems of the older basins are less clearly defined than those of the younger basins. Not all the differences are due to erosion alone, and the following statement holds approximately: The more nearly coincident the basin-forming impact was with the mare epoch, the more pronounced was the resulting radial system. The period leading into the mare epoch was the optimum period for tectonic activity, because (a) temperatures were maximal in subsurface layers, (b) the viscosity was correspondingly lowered in these layers, (c) the surface was stressed due to the expansion prior to the mare epoch (MacDonald, 1961), (d) the surface should have been unstable if there was extensive melting below (Urey, 1955). The first two reasons allowed tectonic adjustments to occur; the last two caused them to occur. The observations are thus compatible with theory. The observations indicate that if the interval between basin formation and mare epoch was long, the likelihood of tectonic activity along radial lines during the mare epoch was lessened.

The origin of the grid systems and of asymmetry and parallelism in the radial systems remains puzzling. They must relate to stress patterns not associated with the basin systems. The most important conclusion reached here in this connection is that the radial systems themselves are independent of the proposed global grid system except for possible local modifications of the former by the latter. This fact is most clearly shown by Orientale and Imbrium. Therefore, lineaments of a symmetric radial pattern centered on basins should be disregarded in discussions of lunar grids and global stresses. Most such discussions to date have ignored this aspect; exceptions are Fielder's recent paper (1963) and the work of Strom (1964). The author agrees with the often-expressed view that the lunar lineaments are internally produced.

During the mare epoch, magma reached the surface in most of the highly-disturbed basins and their fracture systems, and in some other localized areas. Much damage was done to pre-existing surface structures. In view of this hypothesis of an era of strong tectonic activity, also described in Part I (Hartmann, 1963), the following remarks by Dunbar (1963) on pre-Cambrian activity on the earth are of great interest.

"... contemplate the 2,000,000 square miles of granite gneiss that floors the Canadian Shield, and realize that it all came into place as fluid magma, which congealed beneath a cover of older rocks now long since removed by erosion. The relatively small areas of sedimentary formations that lie infolded among these batholiths, as remnants of their former cover, convey the impression that during these primeval eras, *the crust of the Earth was repeatedly broken and largely engulfed in upwellings of molten material that dwarf all post-Cambrian igneous activity.*" [Italics by W. K. H.]

It is doubtful that this represents a true mare epoch on earth, but the analogy to the hypothesized lunar processes is obvious. The rate of crater production did not change much during the mare epoch, as evidenced by the relative constancy of crater number densities on the various surfaces (Shoemaker, Hackman, and Eggleton, 1962). The mare epoch must have occurred early in the moon's history on the following grounds. The moon is generally thought to be at least 4.5 billion years old (Kuiper, 1963; Urey, 1963). In some models calculated by MacDonald (1961) and others, the temperature at a depth of 200 km reaches a rather flat maximum (and at the moon's center, the melting point of iron) in 1 to 2 billion years. But these models assume (a) heat transport by conduction and radiation, (b) homogeneous distribution of radioactive material, and (c) a chondritic composition. Heat transport by convection, concentration of radioactive material near the surface, and the presence of short-lived radioisotopes would raise the subsurface temperature and shorten the time between the moon's formation and the mare epoch. (Mechanisms for producing short-lived isotopes have been discussed, e.g., by Anders and Stevens, 1960, and by Fowler, Greenstein, and Hoyle, 1962.) Therefore, it appears that the mare epoch occurred within the first 1.5 billion years of lunar history. Shoemaker, Hackman, and Eggleton (1962) propose that the crater density on the maria is consistent with a mare age of 4.5 billion years and with a constant flux of meteorites in this period. At this early period, the moon was much closer to the earth, as is known from the theory of tidal evolution, and Baldwin (1963, p. 203) has argued that the elongation of the earthward axis may represent the tidal bulge frozen into the moon's outer layers at the close of the mare epoch with the moon at 39 percent of its present distance. The correctness of the latter two ideas would imply a mare epoch as long ago as the first 0.2 billion years of lunar history.

Throughout the post-mare period, the moon must have appeared substantially as it is now, except

for the addition of some prominent recent ray craters. We observe that the mare surfaces clearly did not undergo major internal disruptions after they formed. The flux of incoming meteorites was much less than in pre-mare time as evidenced by the sparseness of craters on the maria and on the earth. Tectonic activity was negligible in its effect upon large-scale surface structure and the moon was essentially dead. On the earth, we can trace only the most recent fraction of this period because of the continued erosional and tectonic activity of the earth, which has erased its earliest pre-Cambrian structures. Because of this continued activity the presently observed large-scale, tectonic structure of the earth's active crust may be fundamentally different from the dead, impact-scarred lunar surface, and the proposed similarity of the mare basins to ocean basins (von Bülow, 1958, p. 36), or of faults in the Apennines to the San Andreas fault (Fielder, 1963, p. 87) is very questionable.

The history of the moon sketched on these pages is schematically outlined in Figure 2, which is largely self-explanatory. An attempt is made to correlate the three-phase terminology here with the five-phase stratigraphic nomenclature of Shoemaker (1962).

Plate 36.26 schematically outlines the radial lineament systems of the lunar basins as discussed here.

Acknowledgments. Thanks are due to Dr. G. P. Kuiper, Miss Barbara M. Middlehurst, Mr. D. W. G. Arthur, Mr. E. A. Whitaker, and other colleagues at this Laboratory, and to Dr. Spencer R. Titley and Dr. Evans P. Mayo of the Department of Geology for many helpful discussions; and to Dr. Kuiper for critically reading the manuscript. I relied extensively on Mr. Whitaker's help in selection of photographs from the LPL collection, many of which were taken by Mr. Elliot Moore. Some of the rectified negatives were made by Mr. Harold Spradley. The work reported here was supported by the National Aeronautics and Space Administration through Grant NsG 161-61.

General remarks on plates. The following plates are oriented to show the radial structures, usually with the basin direction downward, and thus the orientation with respect to lunar coordinates is variable. Data at the end of each caption identifies those plates which have been rectified by globe projection, and gives original plate number, scale, and colongi-

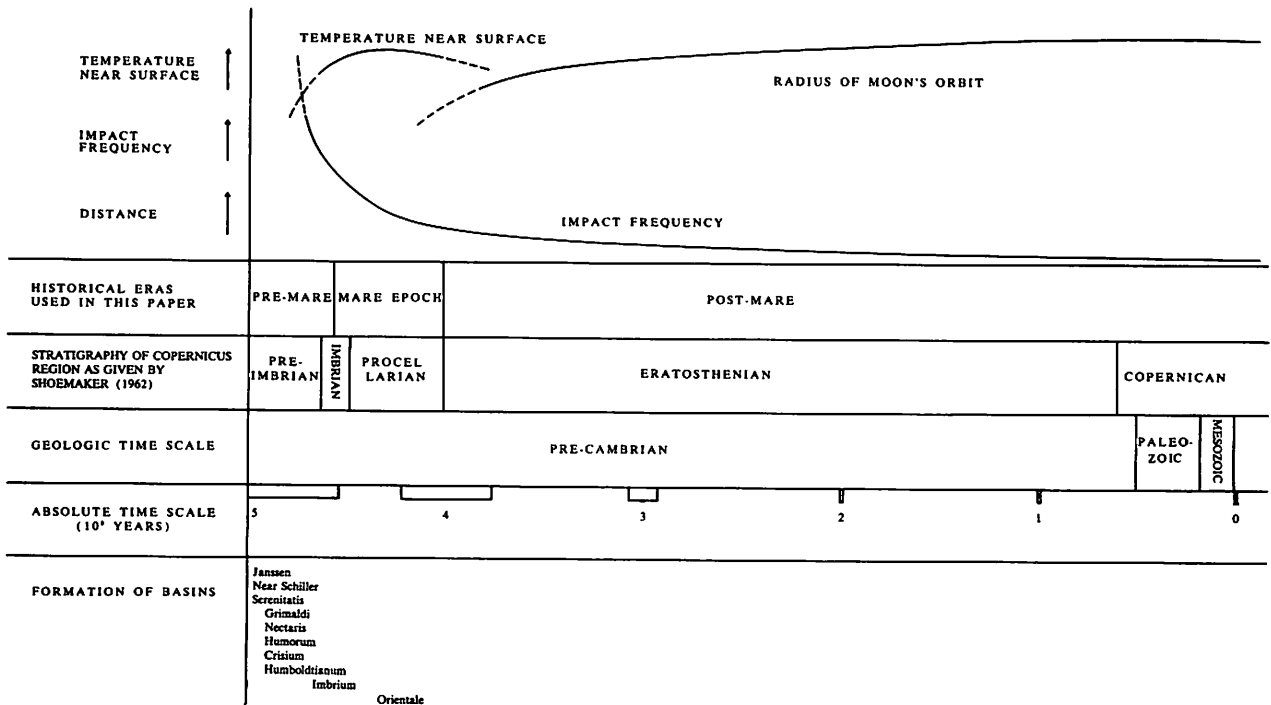


Fig. 2. Simplified schematic outline of lunar history. Various time scales used in geologic and lunar studies are compared. The probable histories of lunar structures, heating, distance, and impact frequency are shown in the upper part of the diagram. The chart illustrates the hypothesis that most of the lunar structures date from a considerably earlier evolutionary stage than is detectable on the earth.

tude of the sun. These plates conclude a long series of photographs specially chosen to illustrate lunar basin systems and published in *Communications of the Lunar and Planetary Laboratory*, Nos. 12, 24, and 36. A catalogue of these photographs is presented in the Appendix.

REFERENCES

- Anders, E., and Stevens, C. M. 1960, *J. Geophys. Res.*, 65, 3043.
- Arthur, D. W. G. 1963, private communication.
- Baldwin, R. B. 1963, *The Measure of the Moon* (Chicago: University of Chicago Press).
- Blagg, Mary A. and Müller, K. 1935, *Named Lunar Formations* (London: Percy Lund, Humphries, and Co., Ltd.).
- Bülow, K. von 1958, *Wiss. Zeitschr. der Univ. Rostock, Math.-Naturwiss. Reihe*, 1, 19.
- Dunbar, Carl O. 1963, *Historical Geology* (New York, Wiley).
- Fielder, G. 1961, *Structure of the Moon's Surface* (New York: Pergamon Press).
- . 1963a, *Nature*, 198, 1256.
- . 1963b, *Quart. J. Geol. Soc. London*, 119, 65.
- Fowler, W. A., Greenstein, J. L., and Hoyle, F. (1962), *Geophys. J.*, 6, 148.
- Gilbert, G. K. 1893, *Bull. Phil. Soc. Washington*, 12, 241.
- Hartmann, W. K. 1963, *Comm. L. P. L.*, 2, 1.
- . 1964, *Comm. L. P. L.*, 2, 197.
- Hartmann, W. K. and Kuiper, G. P. 1962, *Comm. L. P. L.*, 1, 51.
- Kuiper, G. P. 1959, *Vistas in Astronautics*, eds. M. Alperin and H. F. Gregory (London: Pergamon Press), vol. 2.
- . 1963, *Space Science*, ed. D. P. Le Galley (New York: Wiley), chap. 15.
- MacDonald, G. J. F. 1961, *Science*, 133, 1045.
- Rittman, A. 1962, *Volcanoes and Their Activity* (New York: Wiley).
- Sitter, L. U. de 1956, *Structural Geology* (New York: McGraw-Hill Book Co., Inc.).
- Shoemaker, E. M., Hackmann, R. J., and Eggleton, R. E. 1962, in *Advances in the Astronautical Sciences*, 8 (New York: Plenum Press, Inc.).
- Shoemaker, E. M. 1962, *Physics and Astronomy of the Moon*, ed. Z. Kopal (New York: Academic Press, Inc.), chap. 8.
- Spurr, J. E. 1948, *Geology Applied to Selenology* (Lancaster, Pa.: Science Press), vol. 3.
- Strom, R. G. 1964, *Comm. L. P. L.*, 2, 205.
- USAF and NASA 1963, *Lunar Charts* (St. Louis: ACIC).
- Urey, H. C. 1955, *Proc. Nat. Acad. Sci.*, 41, 423.
- . 1961, *Smithsonian Report for 1960*, p. 251.
- . 1963, *Space Science*, ed. D. P. Le Galley (New York: Wiley), chap. 4.
- Vening Meinesz, F. A. 1947, *Trans. A. G. U.*, 28, 1.
- Warner, B. 1961, *J.B.A.A.* 71, 388.
- Whitaker, E. A., Kuiper, G. P., Hartmann, W. K., and Spradley, H. L. 1963 *Rectified Lunar Atlas* (Tucson: University of Arizona Press).

APPENDIX

*Catalog of Lunar Photographs Published in LPL
Communications Nos. 12*, 24**, and 36****

PLATE NUMBER	DESCRIPTIVE TITLE	ORIGINAL	RECTIFIED	APPROXIMATE SCALE km/cm	BASIN INVOLVED
12.1	Mare Crisium, SS	Y 369	X	60	Crisium
12.2	Nectaris Ring System, SR	Y 65	X	56	Nectaris
12.3	Nectaris Ring System, SS	Y 1200	X	56	Nectaris
12.4	Nectaris Ring System, with overlay	Y 65	X	56	Nectaris
12.5	Altai Scarp, SS	W 97	X	56	Nectaris
12.6	Mare Nectaris, SS	Y 1334	X	25	Nectaris
12.7	Mare Nectaris & rilles to N, SR	L 175		25	Nectaris
12.8	Three rings in Nectaris system, SR	Y 65	X	25	Nectaris
12.9	Three rings in Nectaris system, SS	Y 1335	X	25	Nectaris
12.10	Theophilus region, SR	L 193		25	Nectaris
12.11	Theophilus region, SS	W 97		25	Nectaris
12.12	Humorum Ring System, SR	M 694	X	47	Humorum
12.13	Humorum Ring System, SS	M 191	X	47	Humorum
12.14	Humorum Ring System, with overlay	M 191	X	47	Humorum
12.15	W part of Humorum basin	M 694	X	30	Humorum
12.16	Mare Humorum, SR	M 630		30	Humorum
12.17	Rilles and Ridges E of Mare Humorum, SR	M 611		25	Humorum
12.18	Imbrium Ring System, SR	Y 160	X	85	Imbrium
12.19	Imbrium Ring System, SS	W 115	X	90	Imbrium
12.20	W part of Mare Imbrium, SS	W 252	X	43	Imbrium
12.21	E part of Mare Imbrium, SS	W 115	X	43	Imbrium
12.22	W part of Mare Imbrium, SR	Y 163		30	Imbrium
12.23	E part of Mare Imbrium, SR	Y 1267		30	Imbrium
12.24	Imbrium Ring System, with overlay	W 115	X	90	Imbrium
12.25	Imbrium radial lineaments, M. Vaporum	Y 1350	X	45	Imbrium
12.26	Apennines and Archimedes Island	Y 1269		28	Imbrium
12.27	Archimedes Island	W 121		18	Imbrium
12.28	Moon from above Imbrium basin	Y 577	X	22	Imbrium
12.29	Moon from above Orientale basin	Y 1614	X	200	Orientale
12.30	Orientale Ring System, high lighting	Y 1614	X	65	Orientale
12.31	Orientale Ring System, SR	M 74	X	65	Orientale
12.32	Orientale Ring System, SR	M 372	X	65	Orientale
12.33	Orientale Ring System, SR	M 372	X	41	Orientale
12.34	Orientale Ring System, SR	Y 108	X	65	Orientale
12.35	Orientale Ring System, SR	Y 108	X	48	Orientale
12.36a	E part of Orientale Ring System, SR	Y 1502	X	58	Orientale
12.36b	E part of Orientale Ring System, SR	Y 468	X	64	Orientale
12.37	Orientale Ring System, high lighting	M 121		30	Orientale
12.38a	Orientale Ring System, high lighting	M 831		27	Orientale
12.38b	Orientale Ring System, high lighting	Y 1589		27	Orientale
12.38c	Orientale Ring System, high lighting	Y 1578		27	Orientale
12.39a	Orientale Ring System, SR	Y 1614		27	Orientale
12.39b	Orientale Ring System, SR	Y 836		27	Orientale
12.39c	Orientale Ring System, SR	M 74		27	Orientale
12.40	Orientale Ring System, high lighting	Y 1592	X	63	Orientale
12.41	Orientale Ring System, SS	W 172	X	55	Orientale
12.42	Orientale Ring System, with overlay	M 74	X	60	Orientale
12.43	Orientale Ring System, synthesis	(Drawing)		35	Orientale
12.44	Moon from above SE limb basin	Y 1614	X	160	SE Limb Basin
12.45	SE limb basin, SR	Y 1614	X	80	SE Limb Basin
12.46a	SE limb basin, SR	Y 1614		30	SE Limb Basin
12.46b	SE limb basin, SR	Y 1654		30	SE Limb Basin
12.47a	SE limb basin, high lighting	M 831		30	SE Limb Basin
12.47b	SE limb basin, high lighting	M 121		30	SE Limb Basin
12.48	Humboldtianum Ring System, SS	Y 482	X	45	Humboldtianum
12.49	Humboldtianum Ring System, SR	Y 686	X	45	Humboldtianum
12.50	Humboldtianum Ring System, SR	Y 781	X	45	Humboldtianum
12.51	Humboldtianum Ring System, SS	M 30	X	45	Humboldtianum
12.52	Crisium Ring System, SR	Y 784	X	60	Crisium
12.53	Crisium Ring System, with overlay	Y 784	X	60	Crisium
12.54	N part of Crisium Ring System, SR	Y 784	X	40	Crisium

* Concentric Structures Surrounding Lunar Basins

** Radial Structures Surrounding Lunar Basins, I: The Imbrium System

*** Radial Structures Surrounding Lunar Basins, II: Orientale and Other Systems; Conclusions

APPENDIX (Continued)

PLATE NUMBER	DESCRIPTIVE TITLE	ORIGINAL	RECTIFIED	APPROXIMATE SCALE km/cm	BASIN INVOLVED
12.55	N part of Crisium Ring System, SS	Y 369	X	40	Crisium
12.56	W part of Crisium system, SS	Y 1315	X	60	Crisium
12.57a	Maria Marginus and Smythii, high lighting	L 172, 204	X	100	Smythii
12.57b	Maria Marginus and Smythii, high lighting	Lunik III	(X)	100	Marginus
12.58	Maria Marginus and Smythii, SR	Y 686	X	60	Marginus
12.59	Maria Marginus and Smythii, SS	M 479	X	60	Marginus
12.60	Basin near Schiller, SR	Y 1122	X	34	Basin near Schiller
12.61	Basin near Schiller, SR	Y 1011	X	34	Basin near Schiller
12.62	Basin near Schiller, SR	M 694	X	38	Basin near Schiller
12.63	Basin near Schiller, SS	W 171	X	38	Basin near Schiller
12.64	Grimaldi, SR	Y 1502	X	40	Grimaldi
12.65	Grimaldi, SR	Y 108	X	40	Grimaldi
12.66	Grimaldi, SS	Y 1395	X	40	Grimaldi
12.67	Janssen, SS	Y 1335	X	30	Janssen
12.68	Janssen, SS	Y 369	X	38	Janssen
12.69	Janssen, SR	Y 193	X	32	Janssen
12.70	Moon from above S pole	Y 1614	X	150	S Polar (?)
12.71	Leibnitz Mountain arcs	Y 1604	X	65	S Polar (?)
12.72	Bailly and Pingré, SR	Y 1170	X	41	Bailly (?)
12.76	Mare Smythii, high lighting	Y 204	X	65	Smythii
12.77	Full moon with outlines of ring systems	L 224	X	230	All basins
24.1	Moon from above Imbrium basin center	Y 160	X	130	Imbrium
24.2	Looking S from above Mare Imbrium, SS	Y 1350	X	70	Imbrium
24.3	Apennines and Mare Vaporum, SS	Y 1350	X	45	Imbrium
24.4a	Straight Wall, SR	Y 1271		20	Imbrium
24.4b	Straight Wall, SS	W 119		20	Imbrium
24.5a	Cauchy Scarp, SR	L 175		20	Imbrium
24.5b	Cauchy Scarp, SS	W 80		20	Imbrium
24.6	Haemus Mountains, SR	Y 1262		15	Imbrium
24.7	Haemus Mountains, SS	W 111		15	Imbrium
24.8	Apennines and Mare Vaporum, SR	Y 150		30	Imbrium
24.9	Apennines and Mare Vaporum, high lighting	Y 1207		30	Imbrium
24.10	Apennines and Mare Vaporum, SS	W 111		30	Imbrium
24.11	Region of Julius Caesar, SR	Y 744		30	Imbrium
24.12	Region of Julius Caesar, SS	W 111		30	Imbrium
24.13	Region of Ptolemaeus, SR	Pic 34		30	Imbrium
24.14	Region of Ptolemaeus, high lighting	Y 466		30	Imbrium
24.15	Region of Ptolemaeus, SS	W 119		30	Imbrium
24.16	Region of Arzachel, SR	Y 1254		30	Imbrium
24.17	Region of Arzachel, SR	Pic 34		30	Imbrium
24.18	Region of Arzachel, high lighting	Y 466		30	Imbrium
24.19	Region of Arzachel, SS	W 119		30	Imbrium
24.20	Region of Arzachel, with overlay	W 119		30	Imbrium
24.21	Region of Ptolemaeus, with overlay	W 119		30	Imbrium
24.22	Region of Fra Mauro, SR	Y 1267		30	Imbrium
24.23	Region of Fra Mauro, SR	M 285		30	Imbrium
24.24	Region of Fra Mauro, high lighting	Y 466		30	Imbrium
24.25	Region of Fra Mauro, SS	Y 1247		30	Imbrium
24.26	Carpathian Mountains, SR	Y 163		30	Imbrium
24.27	Carpathian Mountains, SS	M 184		30	Imbrium
24.28	Region of Hansteen, SR	M 694	X	45	Imbrium
24.29	Region of Sirsalis Rille, SS	W 230	X	45	Imbrium
24.30	Region of Otto Struve, SR	M 373	X	50	Imbrium
24.31	Western reaches of Mare Imbrium, SR	M 700	X	65	Imbrium
24.32	Vicinity of Aristarchus plateau, SS	W 173	X	50	Imbrium
24.33	Aristarchus plateau, SR	M 700	X	30	Imbrium
24.34	Aristarchus plateau, high lighting	M 184	X	30	Imbrium
24.35	Aristarchus plateau, SS	W 231	X	30	Imbrium
24.36	Region of W. Bond, SR	Y 1350	X	45	Imbrium
24.37	Region of W. Bond, SS	Y 160	X	45	Imbrium
24.38	Region of J. Herschel, SR	M 10	X	40	Imbrium
24.39	Lineaments in Mare Tranquillitatis, SR	Y 72	X	45	Imbrium
24.40	The Imbrium Radial System, with overlay	Y 577	X	180	Imbrium
36.1	Orientele lineaments near Wargentini, SR	Y 108	X	40	Orientele
36.2	Radial lineaments SE of Orientale, SR	Y 1170	X	80	Orientele
36.3	Radial lineaments SE of Orientale, high lighting	Y 1592	X	80	Orientele
36.4	Valleys in and beyond Schickard, SR (120 in.)	Lick 33		10	Orientele
36.5	Lineaments NE of Orientale	M 372	X	50	Orientele

APPENDIX (Continued)

PLATE NUMBER	DESCRIPTIVE TITLE	ORIGINAL	RECTIFIED	APPROXIMATE SCALE km/cm	BASIN INVOLVED
36.6	The Orientale Radial System, with overlay	M 74	X	80	Orientale
36.7	Valleys SE of Nectaris, SS	Y 1310	X	60	Nectaris
36.8	Valleys SSE of Nectaris, SR	L 193	X	60	Nectaris
36.9	Valleys SSE of Nectaris, SS	Y 1200	X	60	Nectaris
36.10a	Extension of Snellius valley toward limb, SR	Y 686	X	80	Nectaris
36.10b	Extension of Snellius valley toward limb, SR	Y 727	X	80	Nectaris
36.11	Valleys ESE of Nectaris, SS	Y 369	X	80	Nectaris
36.12	The Nectaris Radial System, with overlay	Y 482	X	120	Nectaris
36.13	Lineaments SE of Humorum, SS	W 171	X	40	Humorum
36.14	Orthogonal pattern W of Humorum, SR	Y 468	X	40	Humorum
36.15	Orthogonal pattern W of Humorum, SS	W 230	X	40	Humorum
36.16	The Humorum Basin System	W 172	X	80	Humorum
36.17a	Lineaments NW of Crisium, SS	Y 1206	X	50	Crisium
36.17b	Lineaments NW of Crisium, SR	L 175	X	50	Crisium
36.18	Mare Crisium, SR	Y 784	X	45	Crisium
36.19	The Crisium Radial System, with overlay	Y 738	X	80	Crisium
36.20a	Region of Humboldtianum basin, SR	Y 686	X	80	Humboldtianum
36.20b	Region of Humboldtianum basin, SS	L 237	X	80	Humboldtianum
36.21	Region of Humboldtianum basin, SS	Y 482	X	80	Humboldtianum
36.22a	Aristillus, SR	Pic (1945)		30	Humboldtianum
36.22b	Aristillus, SS	W 121		30	Humboldtianum
36.22c	Bullialdus, SS	L 163		30	Humboldtianum
36.22d	Bullialdus, SR	W 171		30	Humboldtianum
36.23a	Copernicus, SR	M (1959)		30	Humboldtianum
36.23b	Eratosthenes, SR	Y 1267		30	Humboldtianum
36.23c	Copernicus, SR	Pic 37b		30	Humboldtianum
36.23d	Aristarchus, SR	M 624		30	Humboldtianum
36.24a	Trough near Aristarchus plateau, SS	W 231		50	Imbrium
36.24b	Trough in Haemus Mountains, SR	W 111		50	Imbrium
36.24c	Trough near W. Bond, SS	Y 1350	X	50	Imbrium
36.24d	Rheita valley, SR	L 193	X	50	Nectaris
36.24e	Valley near Herschel, SS	Y 1261		50	Imbrium
36.24f	Valley in Julius Caesar, SR	W 111		50	Imbrium
36.24g	Mallet Valley, SR	L 193	X	50	Nectaris
36.24h	Valley W of Ptolemaeus, SR	Y 1261		50	Imbrium
36.25a	Orthogonal lineaments near Archimedes, SS	W 115		50	Imbrium
36.25b	Orthogonal lineaments near Macrobius, SR	L 175	X	50	Crisium
36.25c	Orthogonal lineaments near Schickard, SR	W 230	X	50	Humorum
36.25d	Scarp radial to Humboldtianum, SS	Y 482	X	50	Humboldtianum
36.25e	Scarps radial to Nectaris, SR	L 193	X	50	Nectaris
36.25f	Scarps radial to Orientale, SR	Y 1170	X	50	Orientale
36.25g	Damaged crater Réaumur, SR	Y 1261		50	Imbrium
36.25h	Damaged crater Parry M, SR	Y 557		50	Imbrium
36.25i	Damaged crater in Palus Epedemaiaurum, SS	W 171	X	50	Humorum
36.36	Radial and concentric basin systems	L 224		190	All basins



Plate 36.1. Radial system of Mare Orientale in the region of Wargentín, Schickard, and Inghirami, viewed from above Mare Orientale. South is up; cf. Plate 36.2. Rectified; Y108; scale ~ 4.0 km/mm (1:4,000,000); col. 78°8.

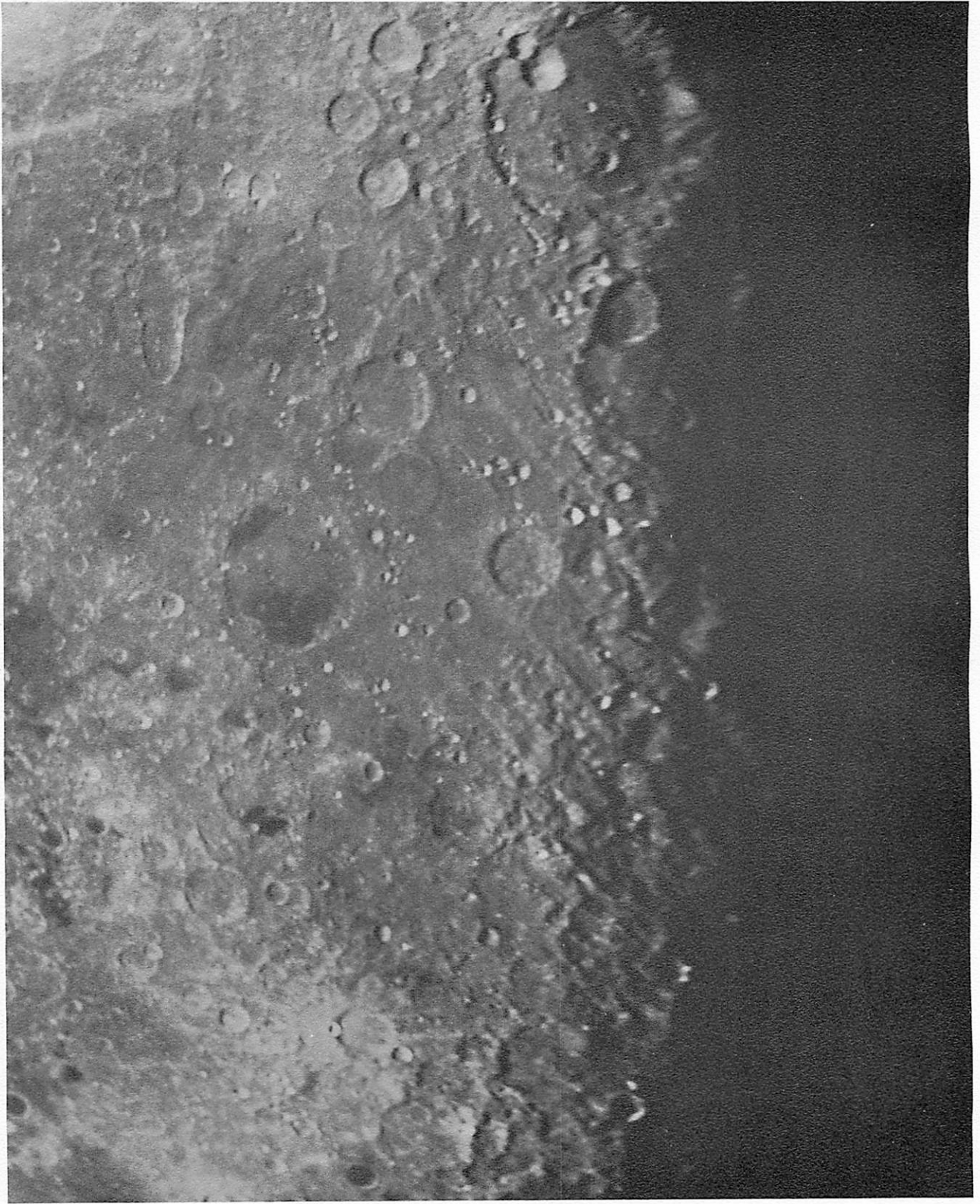


Plate 36.2. Radial system, extending SE from Mare Orientale. Many scarps and valleys are prominent. Compare with Plate 36.3 of same region in full sunlight. Rectified; Y1170; scale ~ 8.0 km/mm (1:8,000,000) col. 82°1.

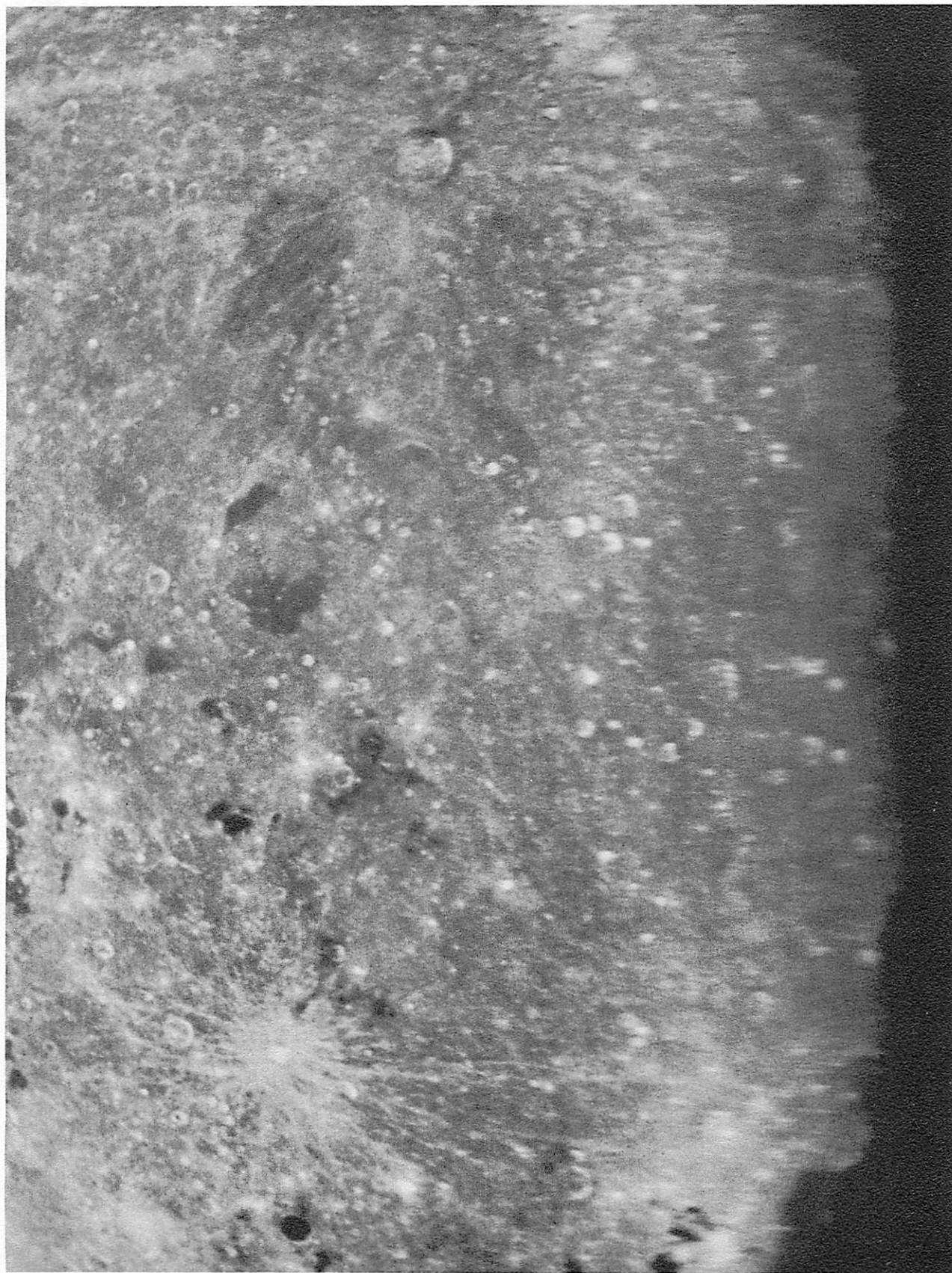


Plate 36.3. Same region at high lighting, showing lack of distinguishing photometric properties of radial structures. Rectified; Y1592; scale ~ 8.0 km/mm (1:8,000,000); col. 120°3.



Plate 36.4. Valleys radial to Mare Orientale in and beyond Schickard. Valleys on the far floor of Schickard appear softened or buried. Compare those beyond Wargentín. Not rectified, Lick 120-inch, no. 33; scale ~ 1.0 km/mm (1:1,000,000); col. 67:8 (Courtesy Lick Observatory).

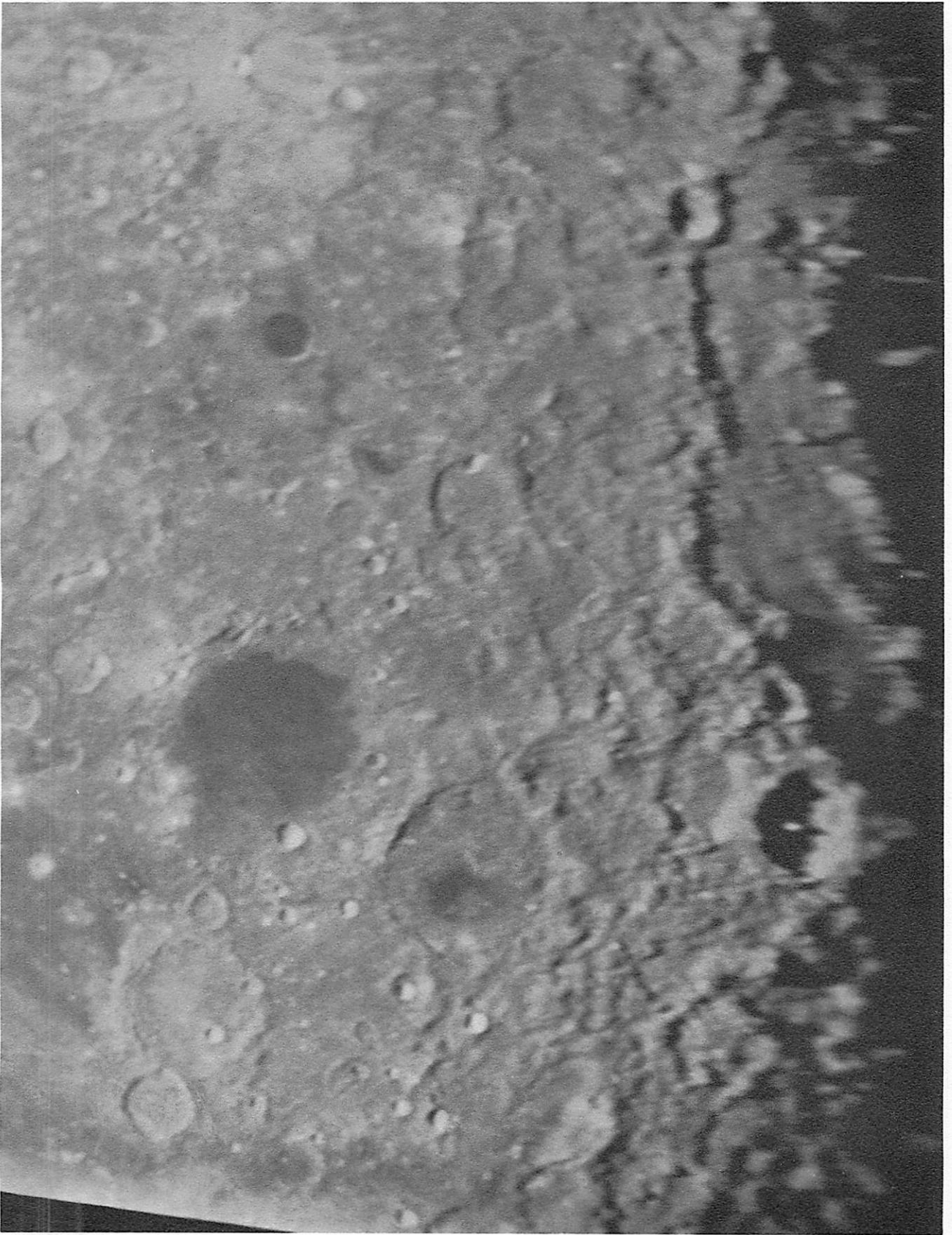


Plate 36.5. Region from E to N of Mare Orientale. Nearly orthogonal lineament pattern is prominent NE of basin. Rectified; M372; scale ~ 5.0 km/mm (1:5,000,000); col. 85:7.

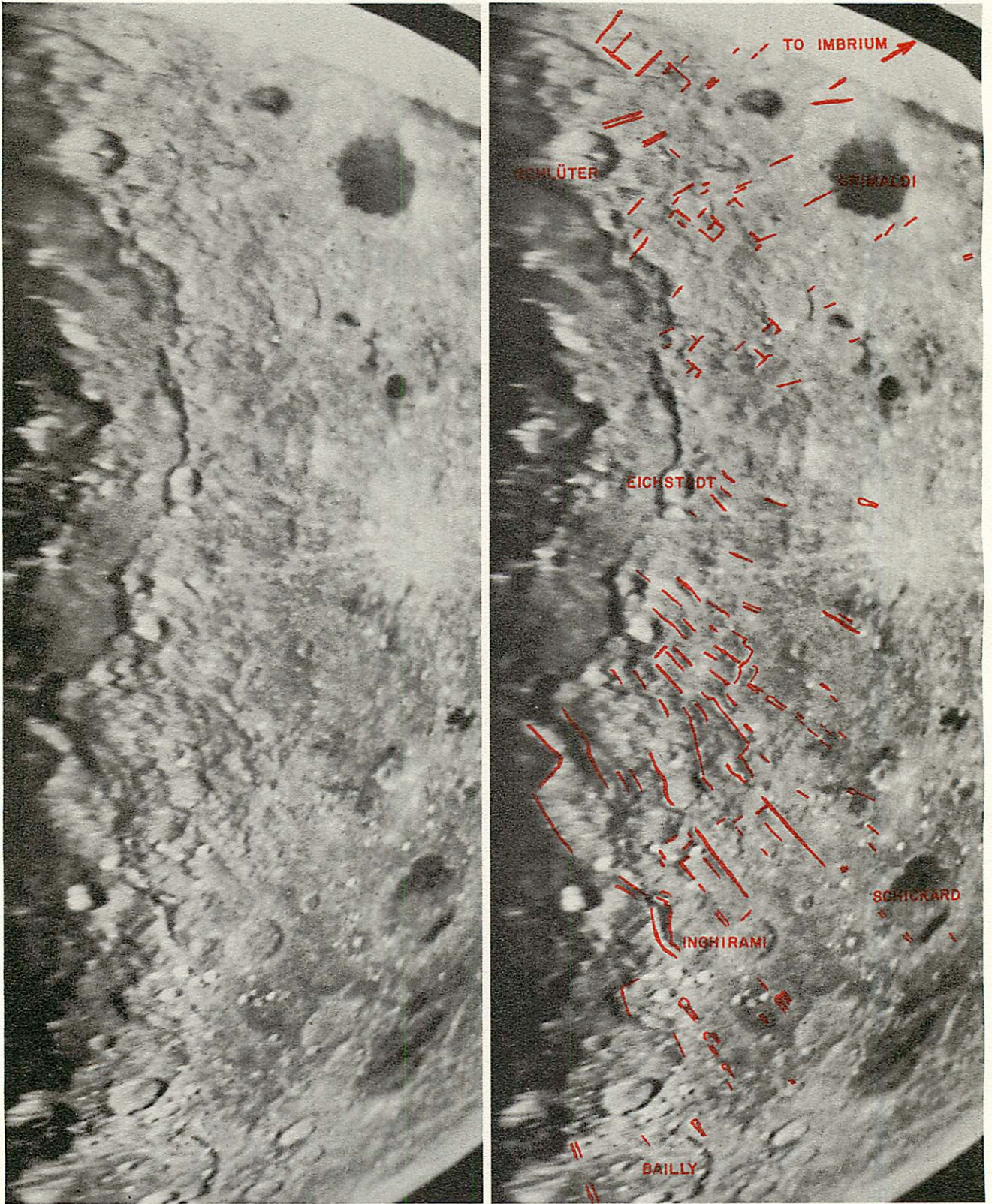


Plate 36.6. The Orientale basin system from an effective altitude of 4900 km above the surface. Overlay marks the most prominent members of the radial system. The concentric rings are clearly defined. Rectified; M74; scale ~ 8.0 km/mm (1:8,000,000); col. 88:9.

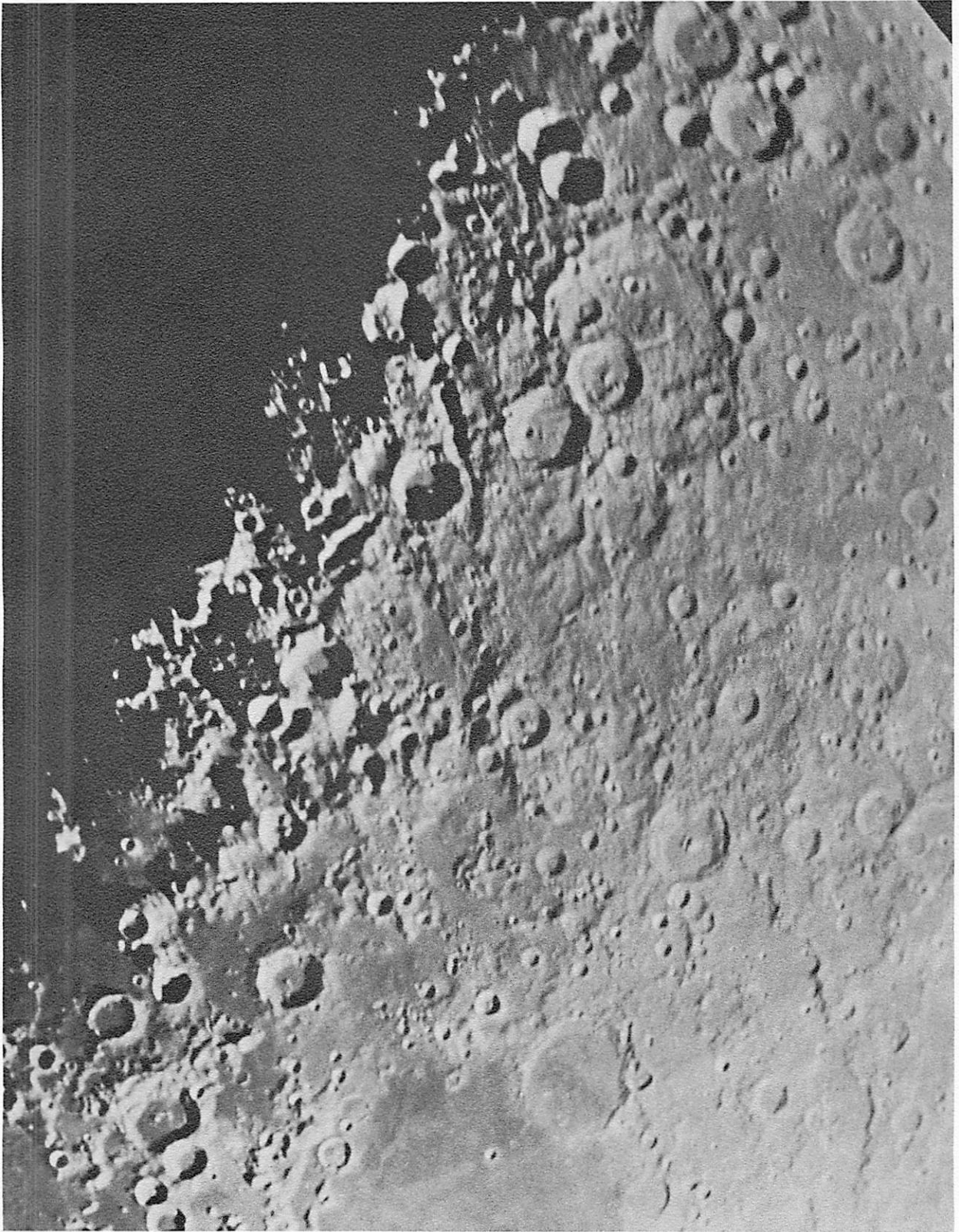


Plate 36.7. Low sun on the region SE of the Nectaris basin. Rheita Valley and W end of Snellius Valley are visible. For map and nomenclature of valleys, see Plate 36.12. Rectified; Y1310; scale ~ 6 km/mm (1:6,000,000); col. 127:1.

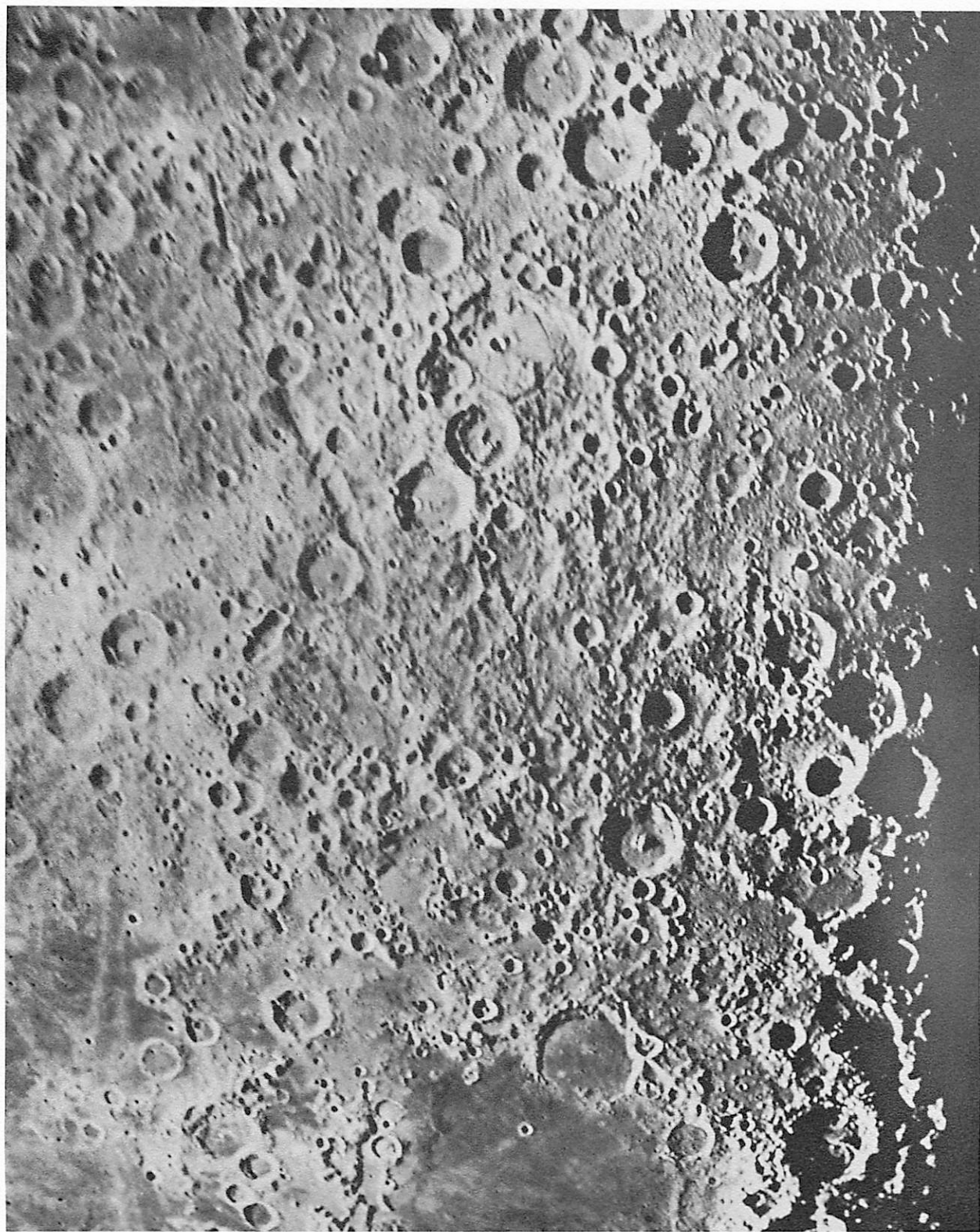


Plate 36.8. Valleys and other lineaments SSE of the Nectaris basin under sunrise lighting. Compare Plate 36.9 at same scale and orientation. Rectified; L193; scale ~ 6.0 km/mm (1:6,000,000); col. 338°9.

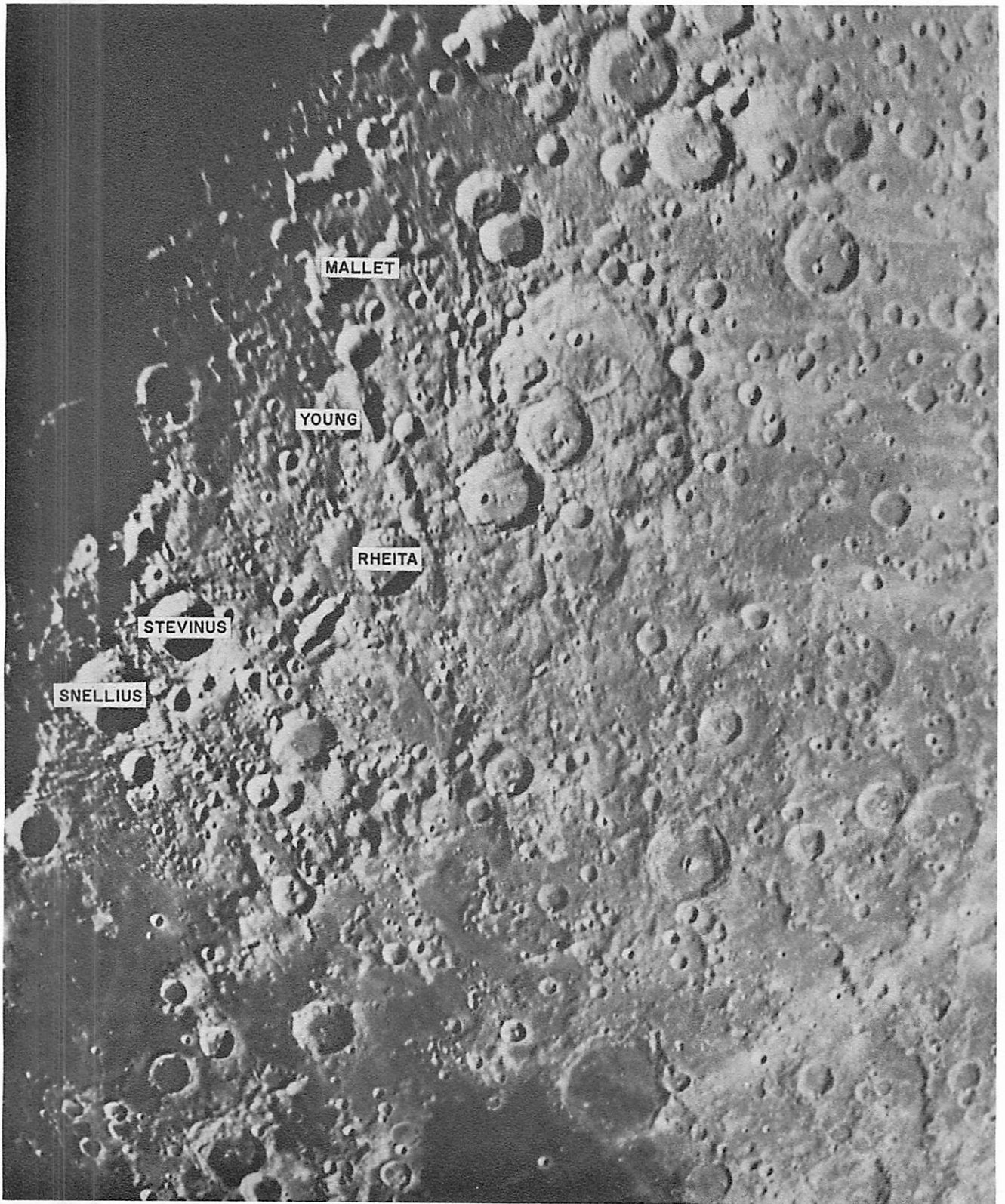
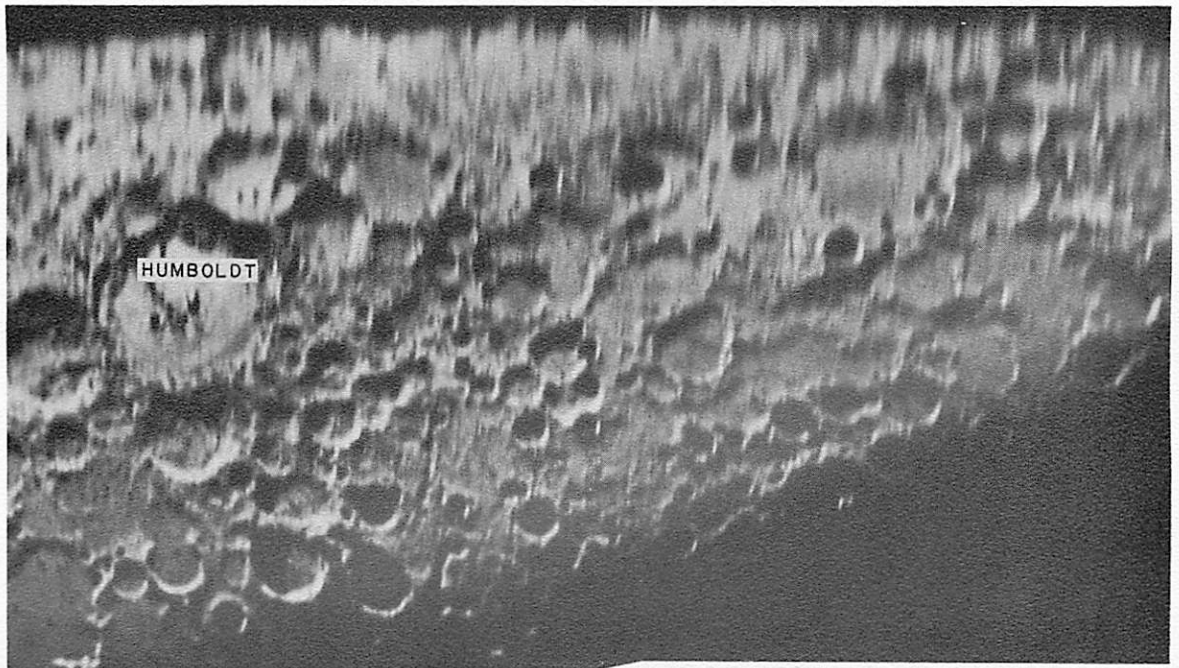
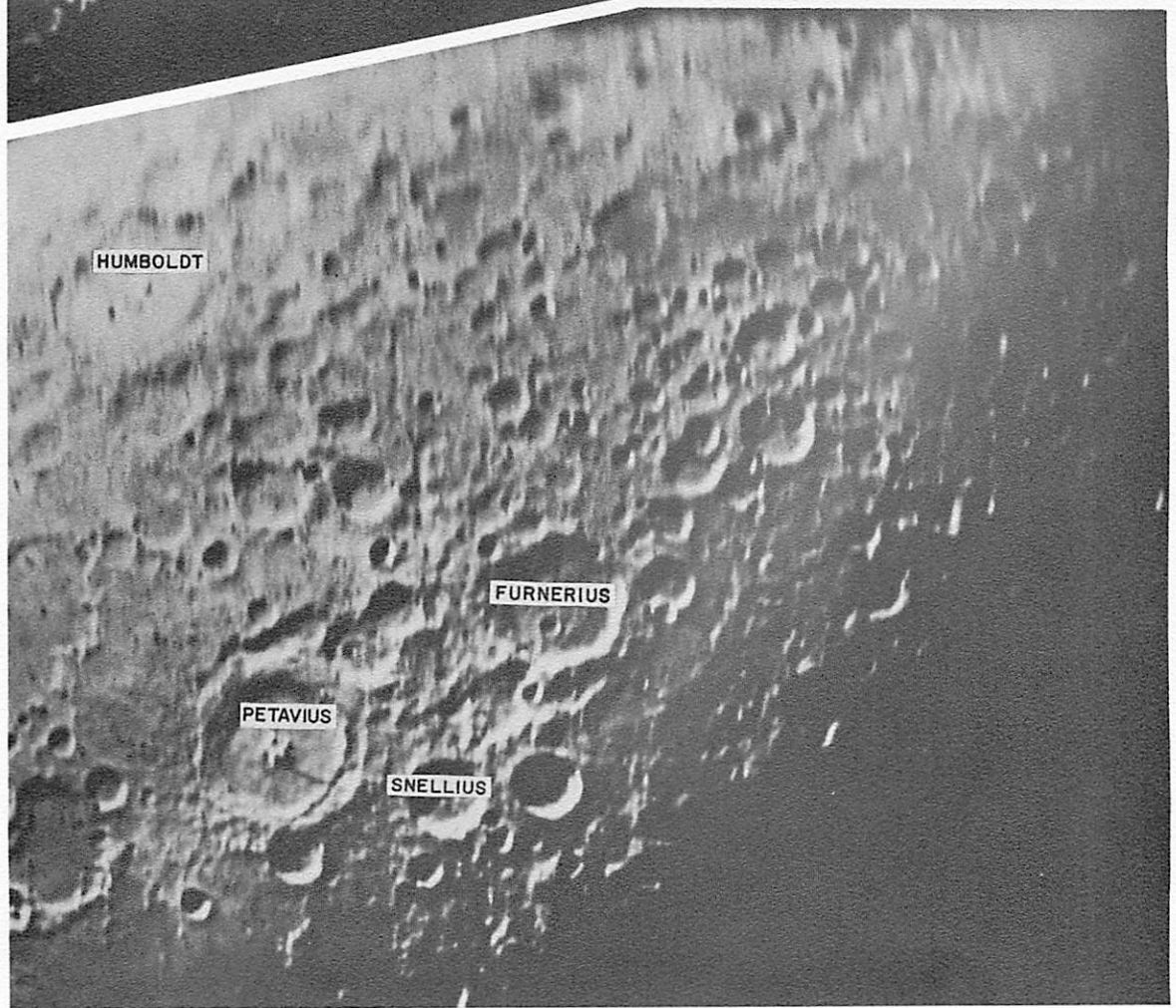


Plate 36.9. The same area under sunset lighting. Cf. Plate 36.8 at same scale and orientation. Rectified; Y1200; scale ~ 6.0 km/mm (1:6,000,000); col. 120°2.



(a)



(b)

Plate 36.10. The limb ESE of the Nectaris basin, showing the eastward, *en échelon*, extension of the Snellius Valley. Total length of this valley is some 800 km. Cf. facing Plate 36.11. (a) Rectified; Y686; scale ~ 8 km/mm (1:8,000,000); col. 294:4. (b) Rectified; Y727; scale ~ 8 km/mm (1:8,000,000); col. 311:9.

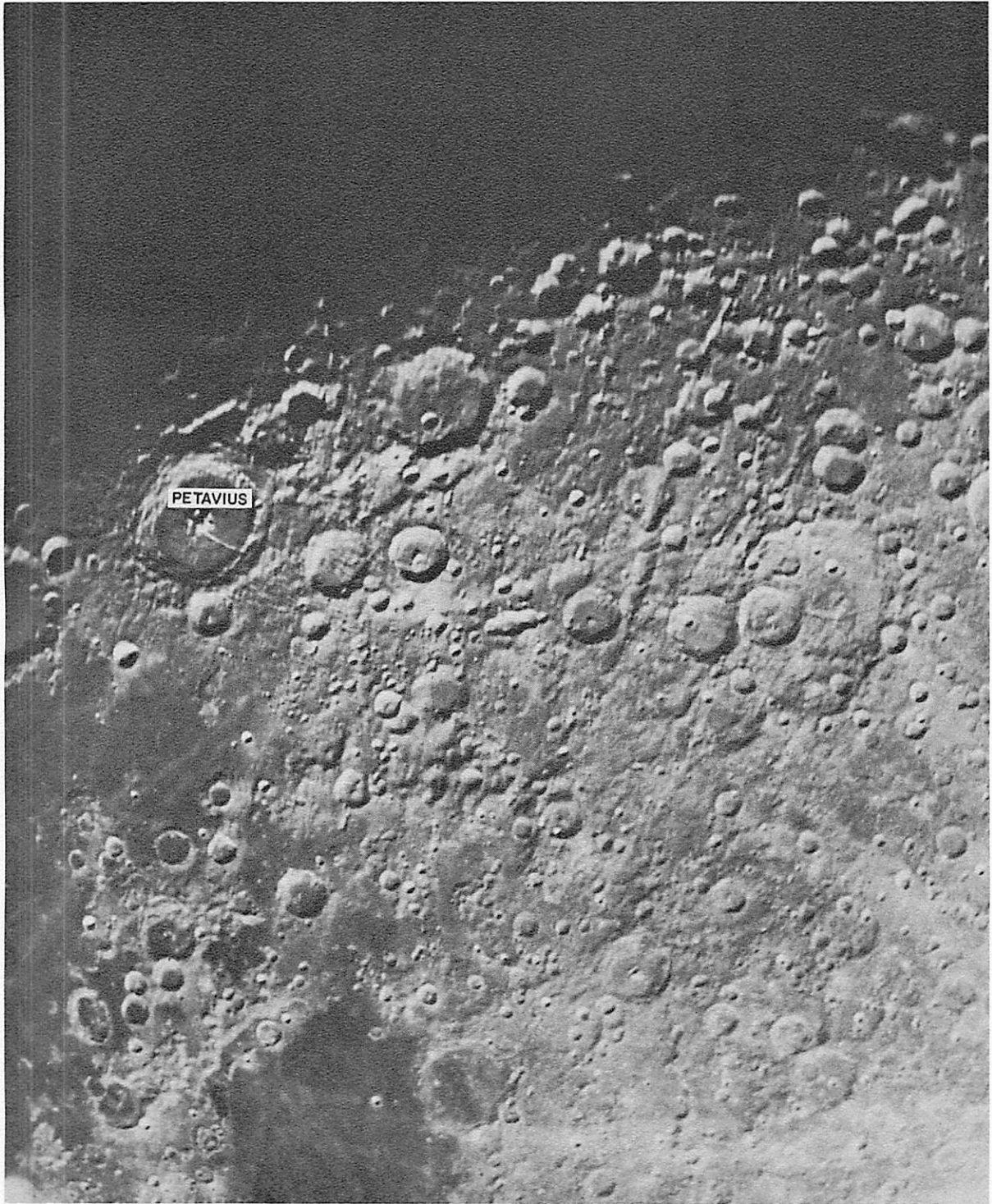


Plate 36.11. Region of major valleys ESE of the Nectaris basin. The W part of the Snellius Valley, running between Petavius and Furnerius, is well seen. Cf. Plate 36.10 for the eastward extension of this area. Rectified; Y369; scale ~ 8 km/mm (1:8,000,000); col. 113°1.

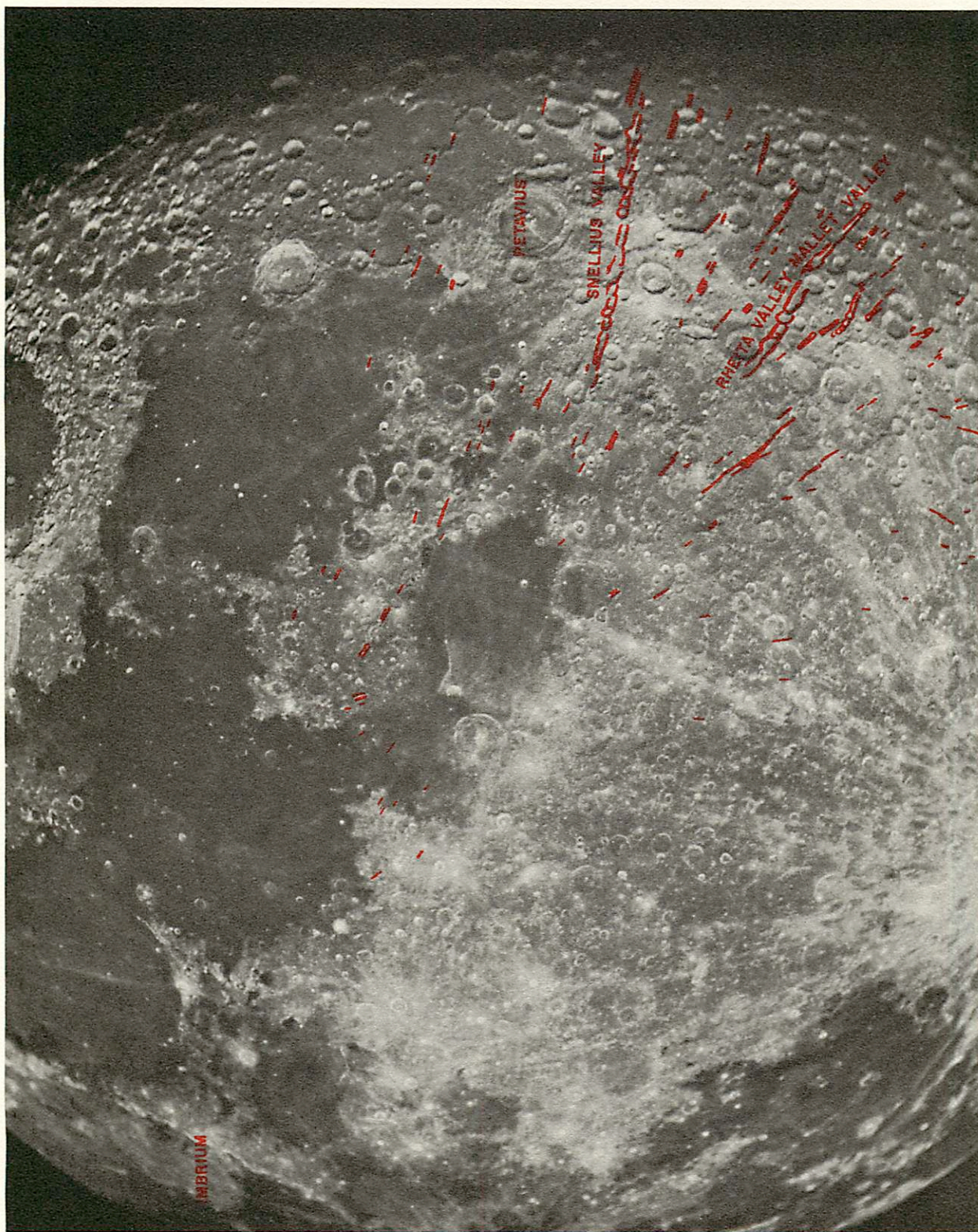


Plate 36.12. The Nectaris basin system. Overlay marks the most prominent lineaments, many converging toward a center in the Nectaris inner basin. In addition, it can be seen that the Imbrium radial pattern extends into this region. Rectified; Y482; scale ~ 12 km/mm (1:12,000,000); col. 100°8.

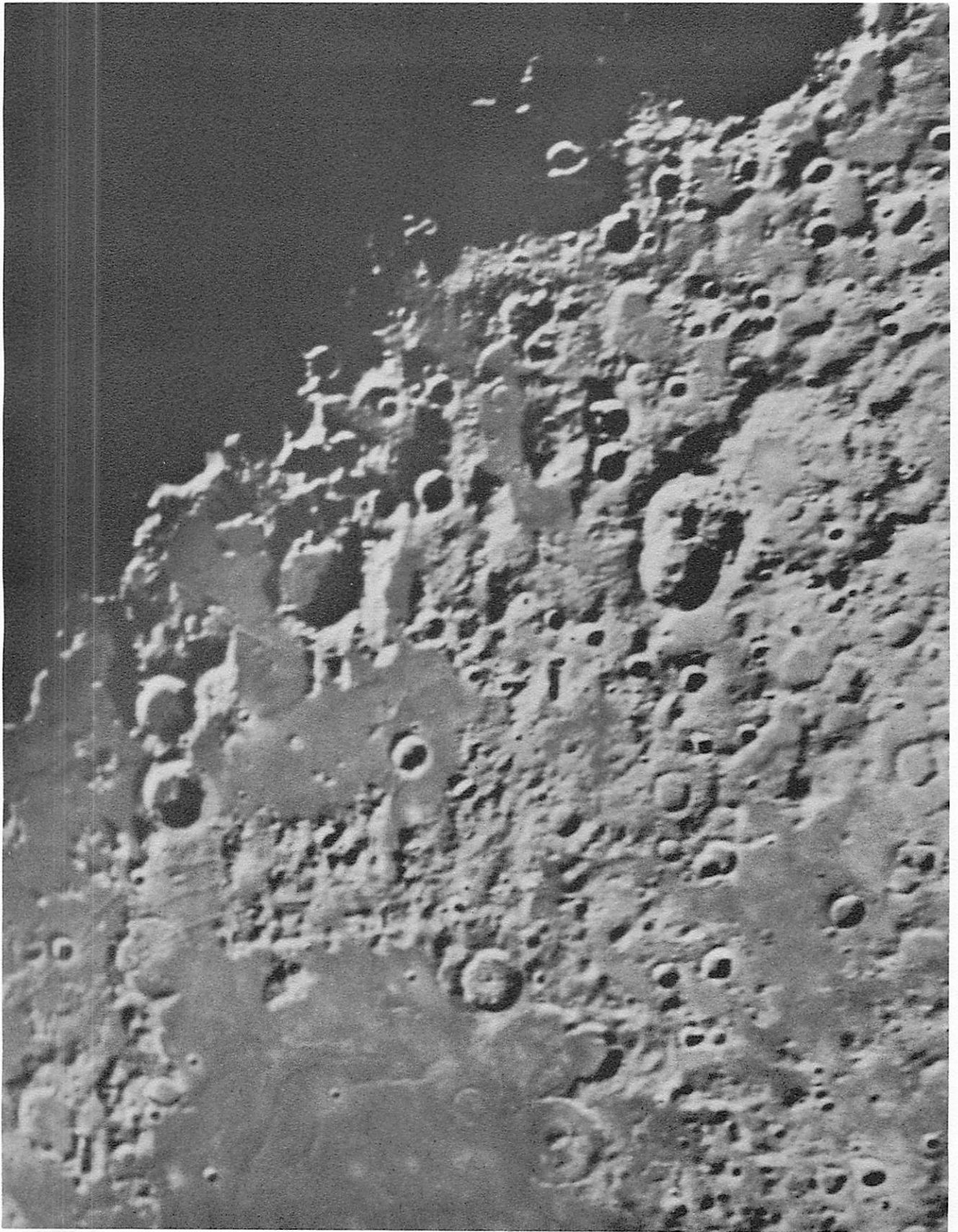


Plate 36.13. Region SE of the Humorum basin. A lineament pattern running vertically through the photograph may be recognized. Rectified; W171; scale ~ 4.0 km/mm (1:4,000,000); col. 202°6.

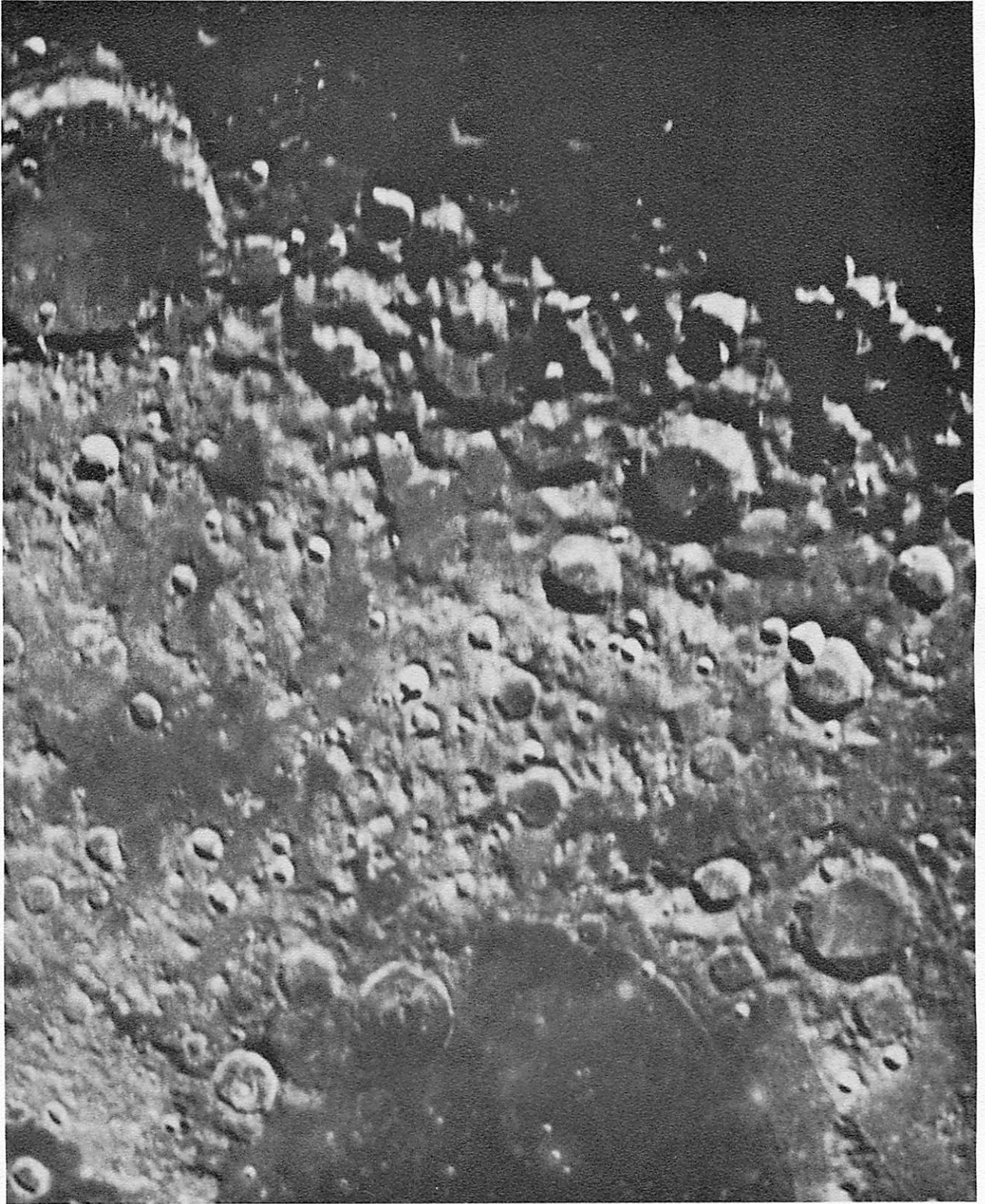


Plate 36.14. Orthogonal lineament pattern W of the Humorum basin, sunrise. Upper central part of photograph shows a region of damaged craters, ridges, and apparent rectilinear faults. Radial patterns also evident closer to the inner basin. Cf. facing Plate 36.15. Rectified; Y468; scale ~ 4.0 km/mm (1:4,000,000); col. 63°1.

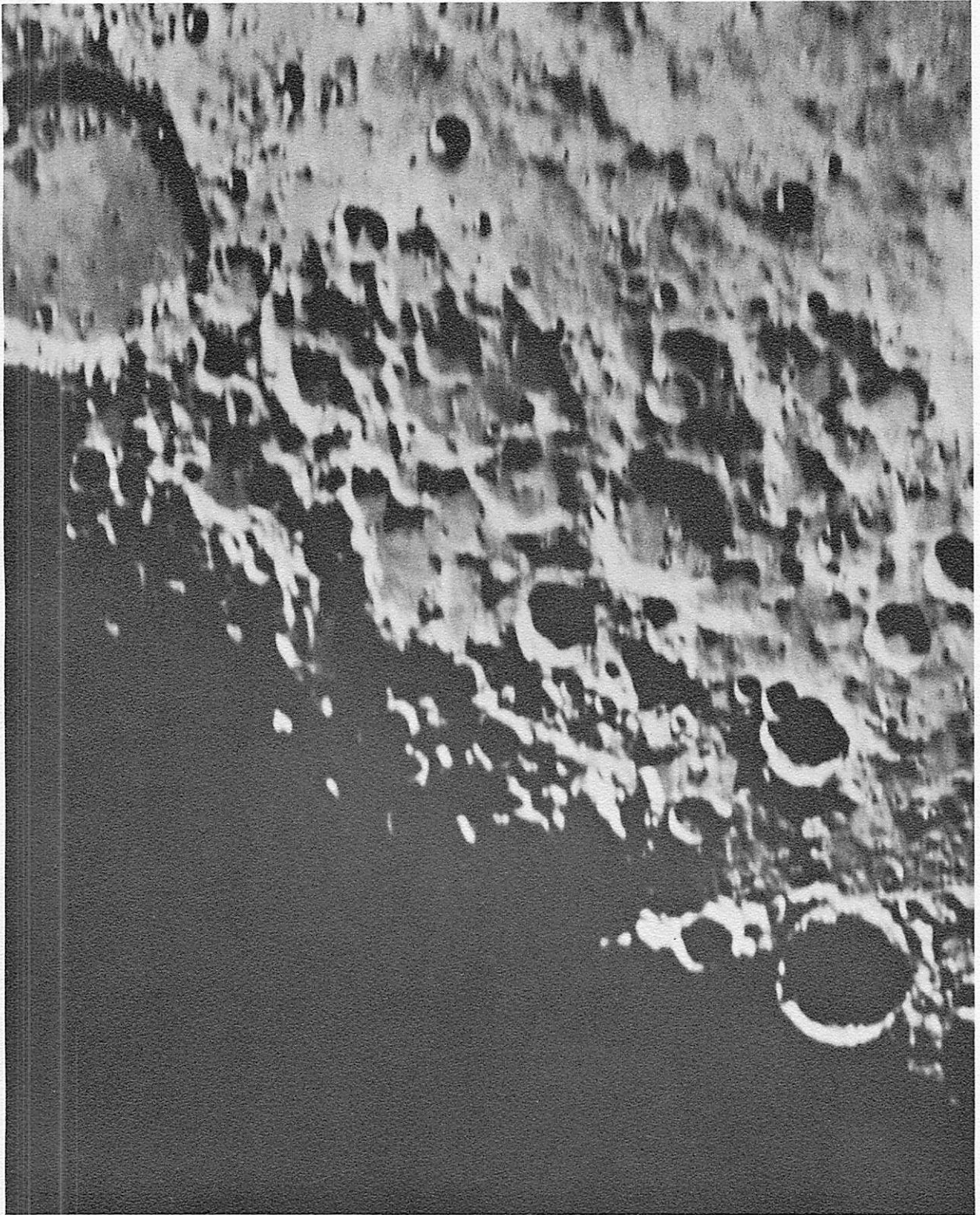
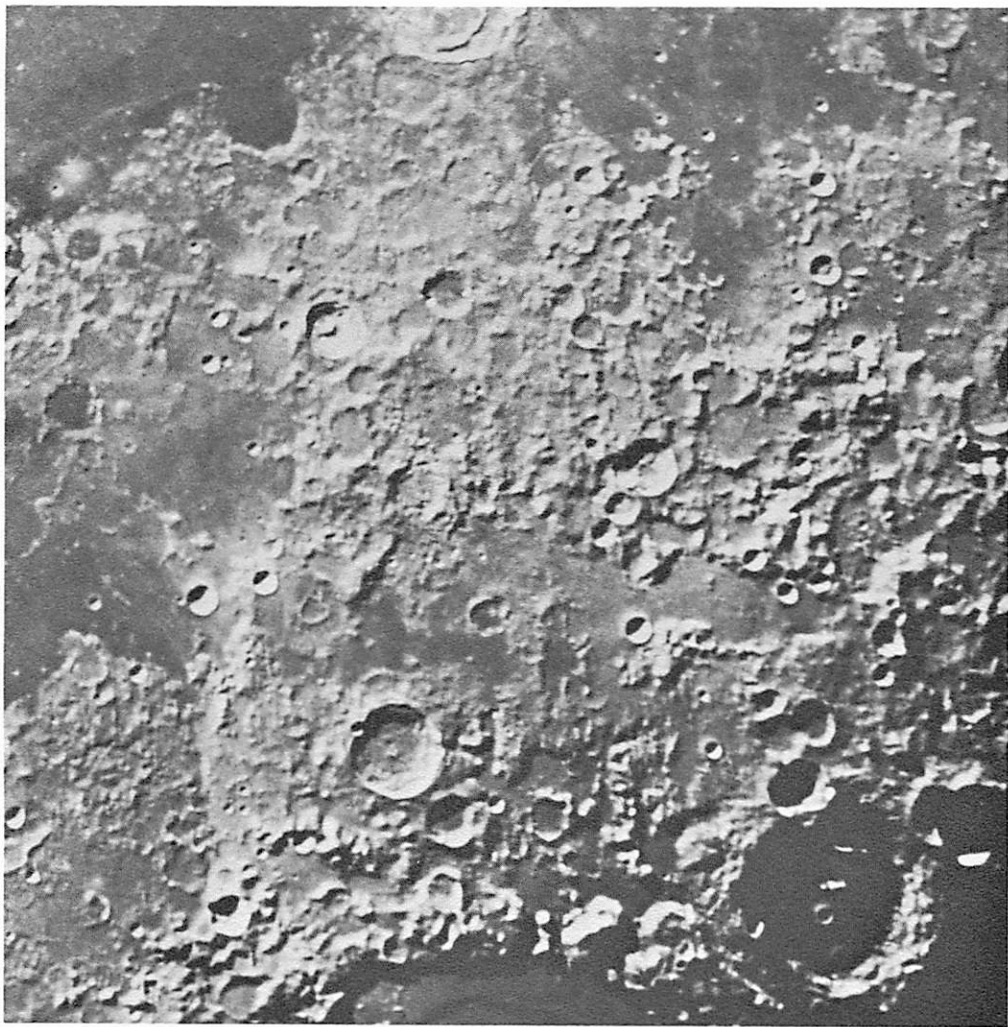


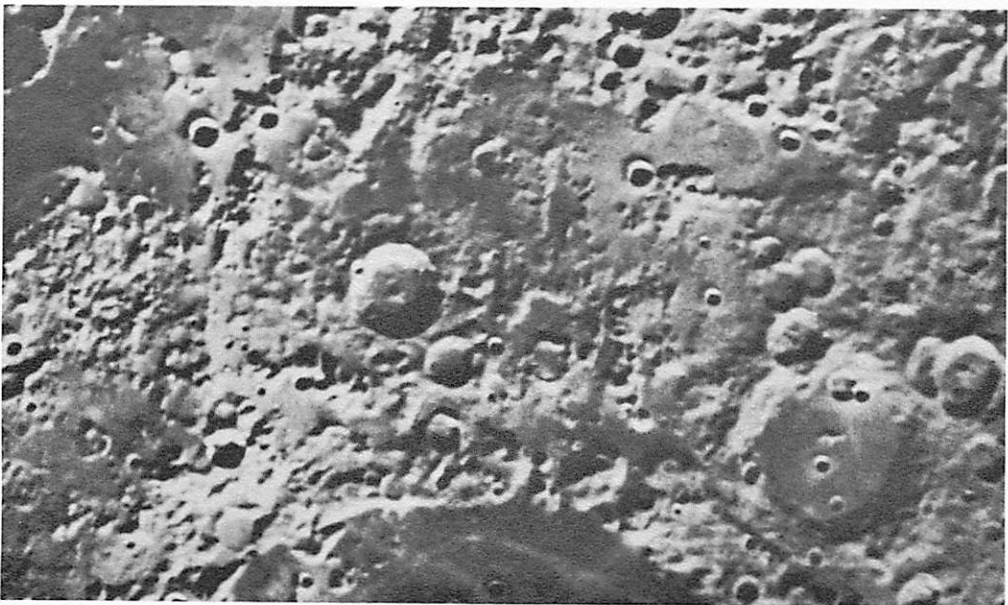
Plate 36.15. Same as Plate 36.14, sunset. This shows that the region has been partially flooded. Rectified; W230; scale ~ 4.0 km/mm (1:4,000,000); col. 229°1.



Plate 36.16. The Humorum basin system. The tendency for local parallelism can be seen. Dashed lines show directions to Imbrium center and Orientale center. Rectified; W172; scale ~ 8.0 km/mm (1:8,000,000); col. 202°6.



(a)



(b)

Plate 36.17. Lineaments NW of the Crisium inner basin, between the two major rings of the concentric system. Note the juxtaposition of the local flooding and the lineaments. (a) Rectified; Y1206; scale ~ 5.0 km/mm (1:5,000,000); col. 120:5; (b) rectified; L175; scale ~ 5.0 km/mm (1:5,000,000); col. 328:7.

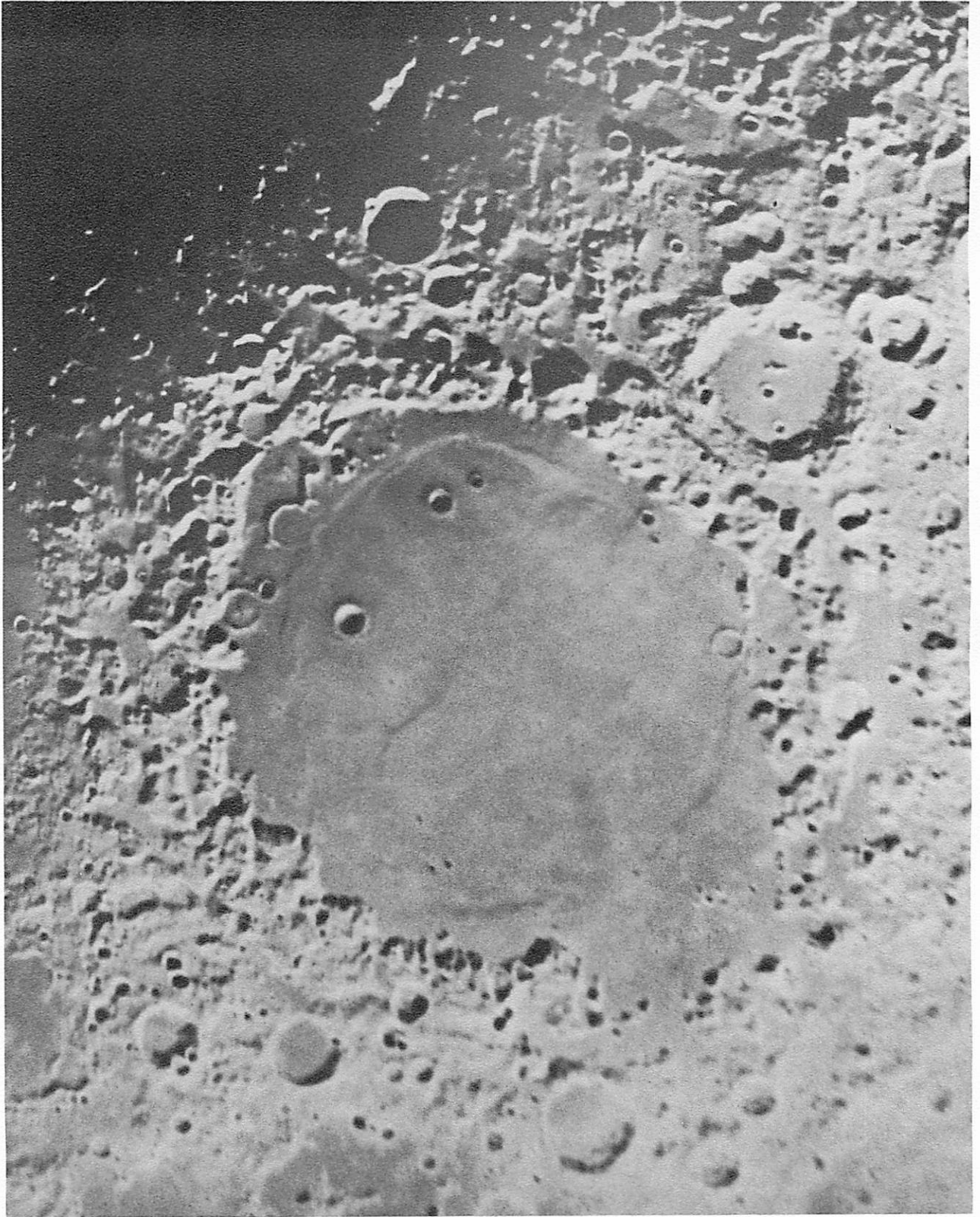


Plate 36.18. Mare Crisium at sunrise. Note step-pattern of lineaments in NW wall (lower left). Rectified; Y784; scale ~ 4.5 km/mm (1:4,500,000); col. 317:1.

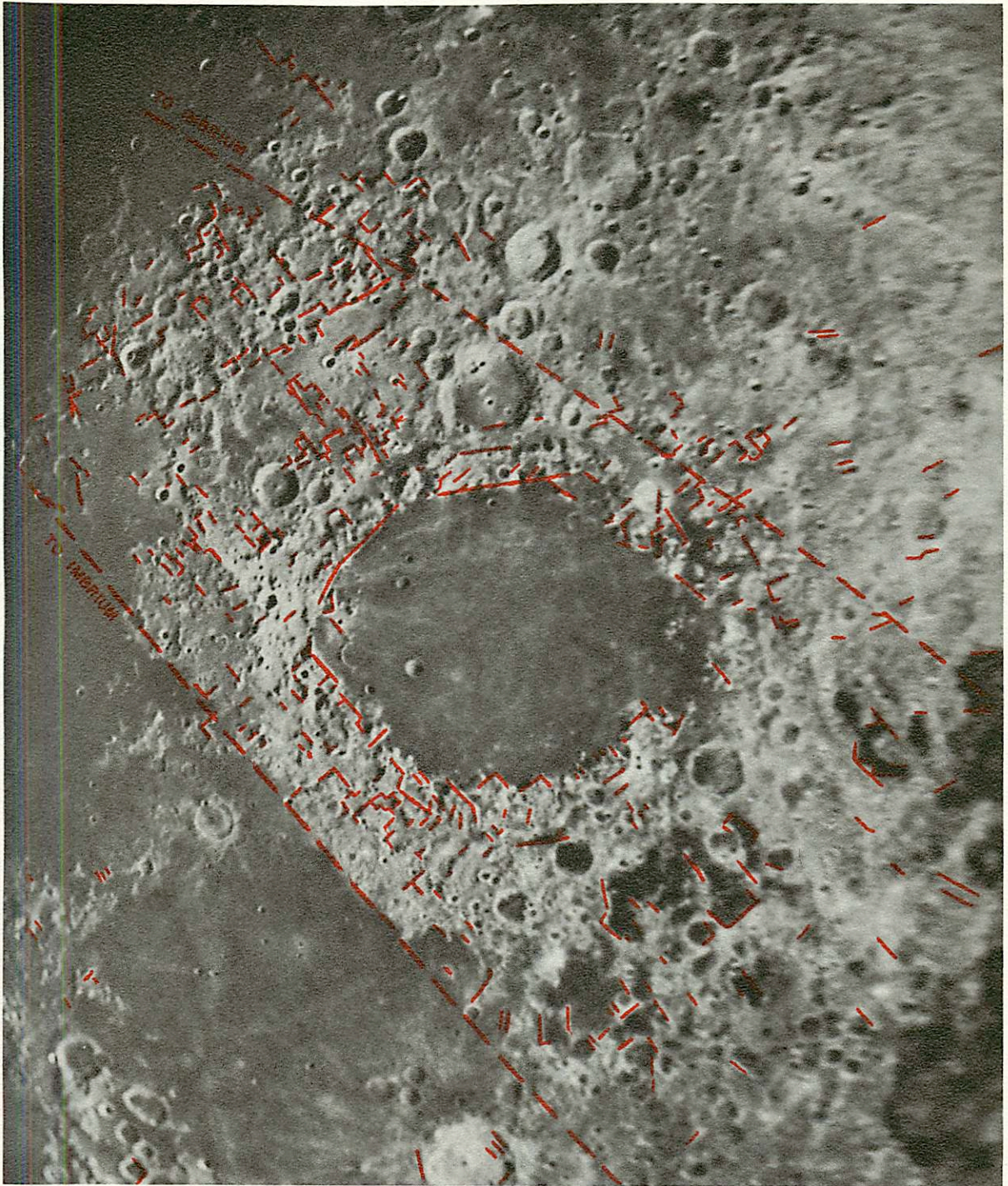


Plate 36.19. The Crisium basin system, showing prominent lineament patterns. The lack of complete symmetry with the Imbrium basin rules out the possibility that all these are outlying members of the Imbrium system. Rectified; Y738; scale ~ 8.0 km/mm (1:8,000,000); col. 337°5.



(a)



(b)

Plate 36.20. Environs of the Humboldtianum basin. Plate (a) shows the "ghost scarps" between Humboldtianum and Crisium. Compare facing plate. (a) Sunrise; rectified; Y686; scale ~ 8.0 km/mm (1:8,000,000); col. 294:4; (b) sunset; rectified; L237; scale ~ 8.0 km/mm (1:8,000,000); col. 87:8.

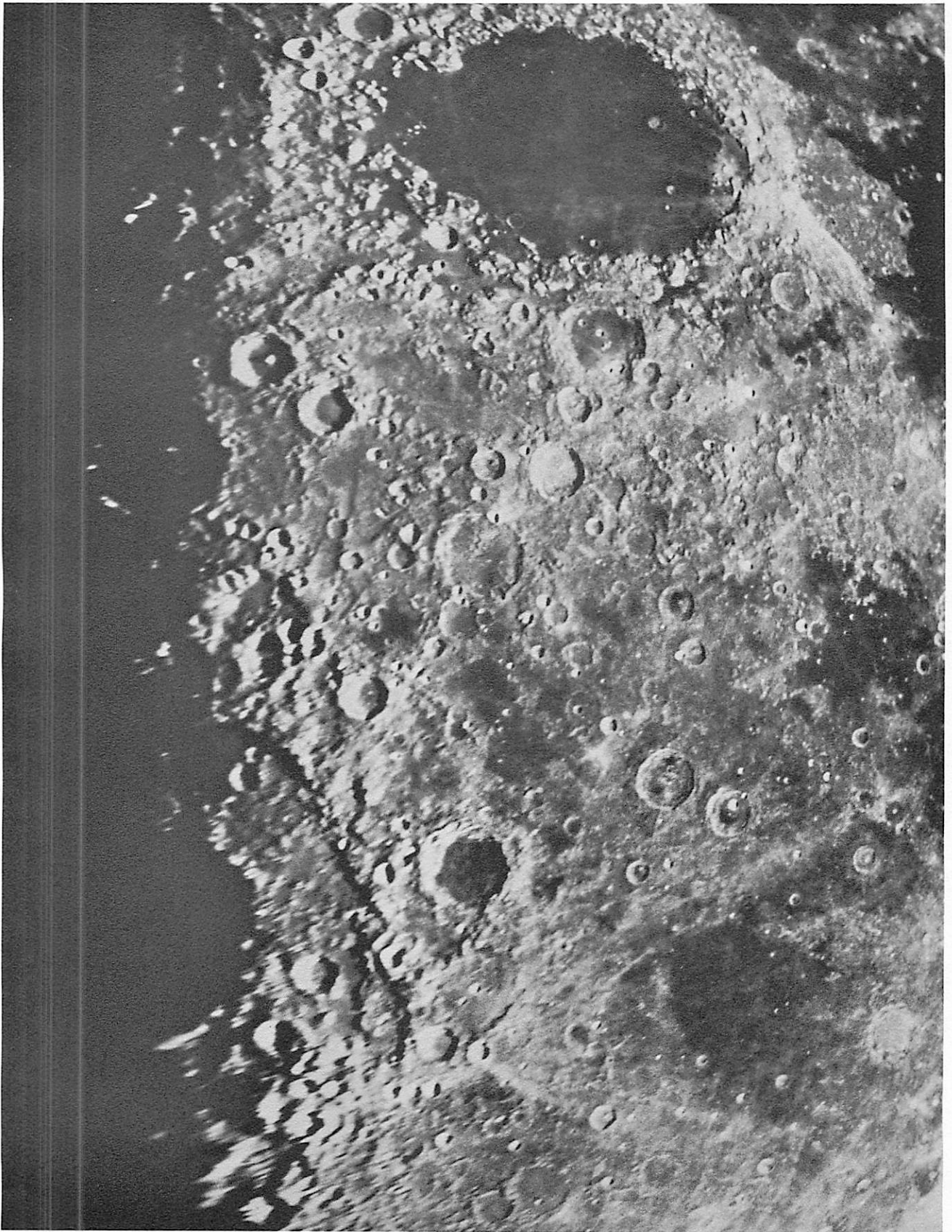
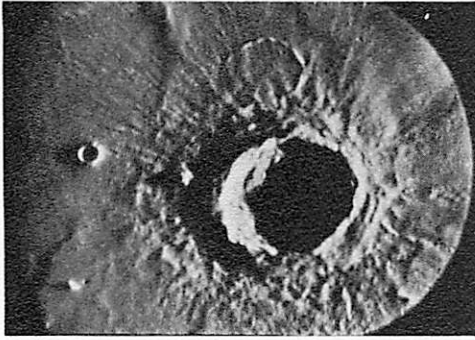
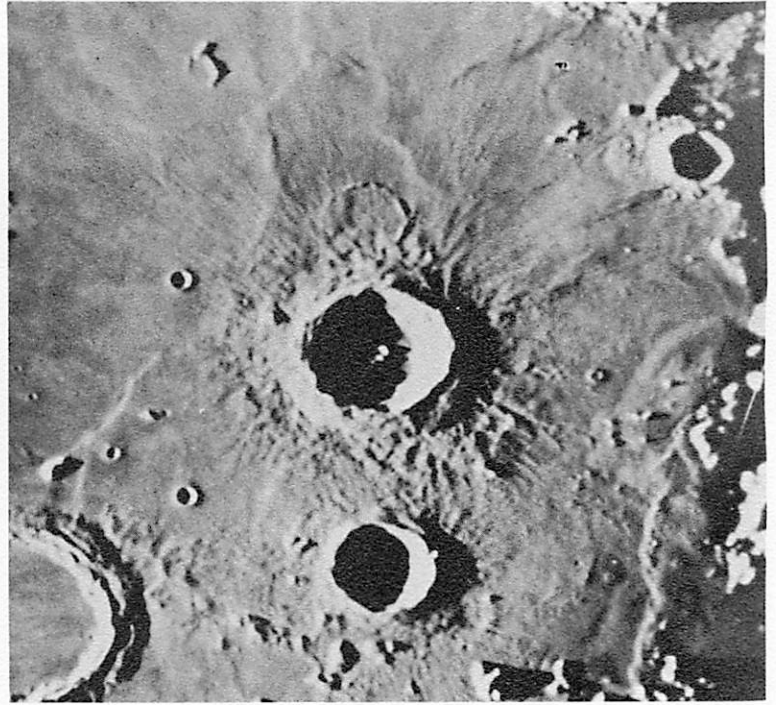


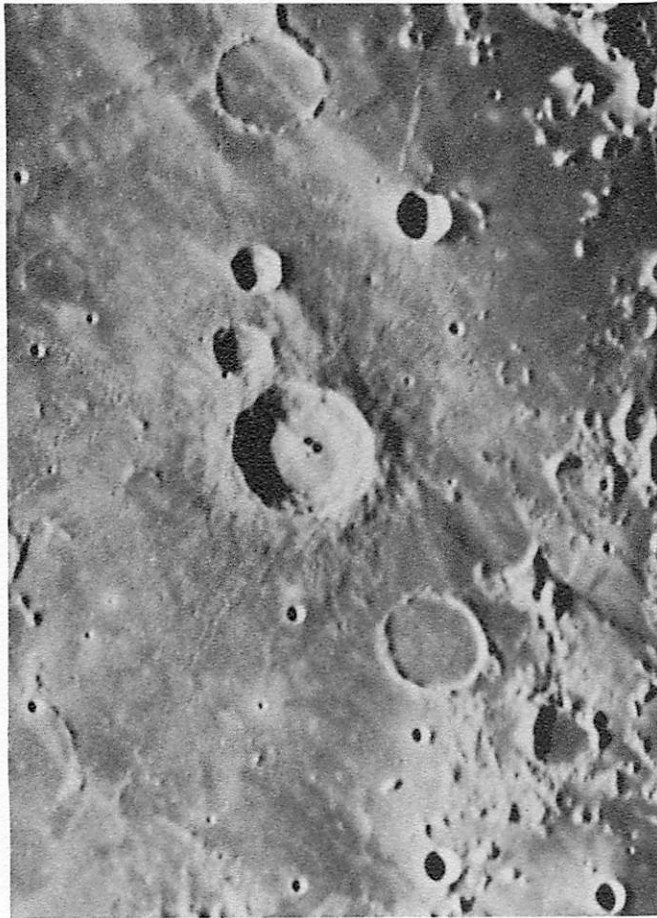
Plate 36.21. Environs of the Humboldtianum basin. The two "ghost scarps" between Crisium and Humboldtianum are well shown. Between the inner and outer rings of the Humboldtianum basin system is a radial scarp, apparently bordered on the lower side by patches of maria, as seen on facing Plate 36.20b. Rectified; Y482; scale ~ 8.0 km/mm (1:8,000,000); col. 100°8.



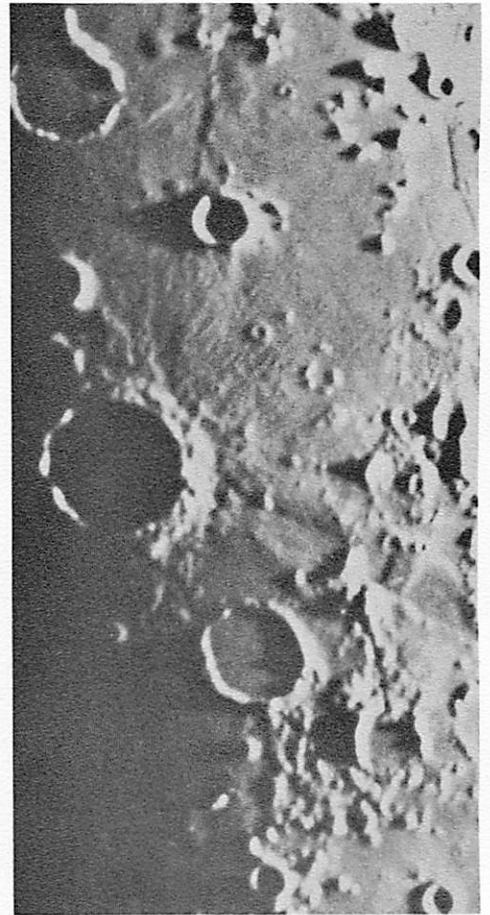
(a)



(b)

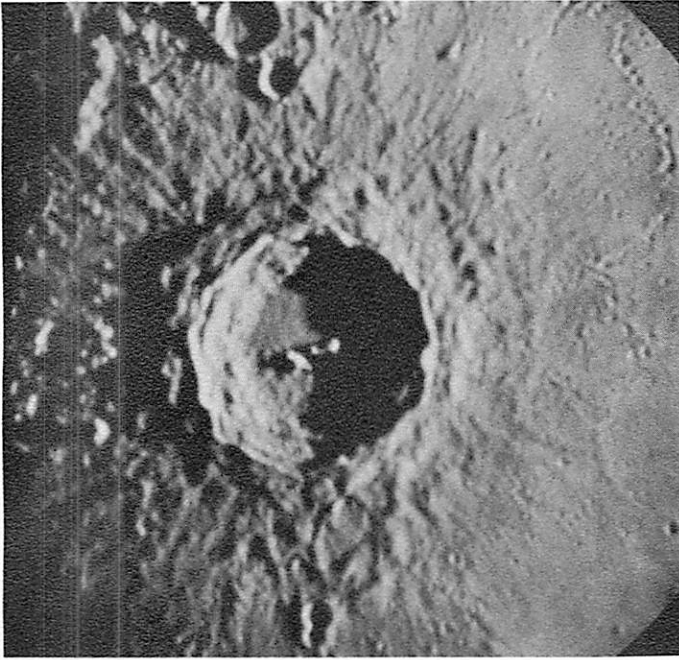


(c)

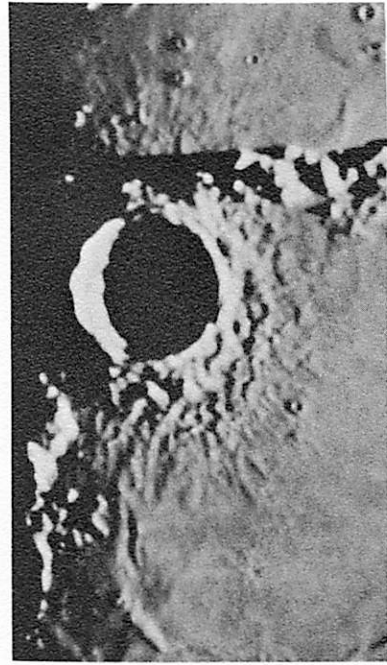


(d)

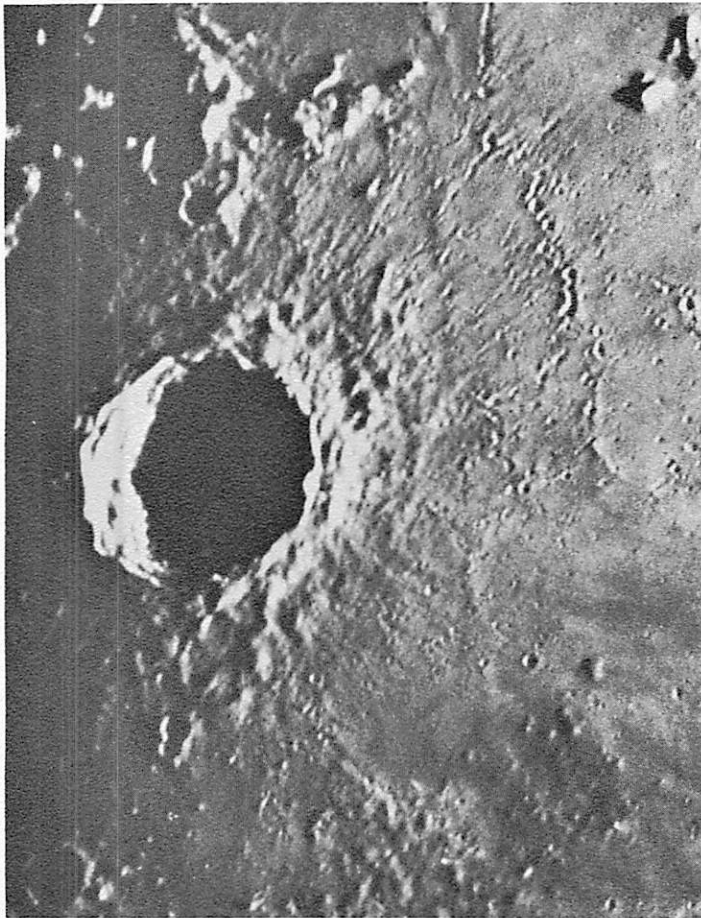
Plate 36.22. Four photographs of radial systems around craters. These lineaments are finer and of different character than those around basins. Scale ~ 3 km/mm. (a) Aristillus; Pic du Midi, Mar. 21, 1945; col. 6°2; (b) Aristillus; W121; col. 172°1; (c) Bullialdus; L163; col. 38°2; (d) Bullialdus; W171; col. 202°6.



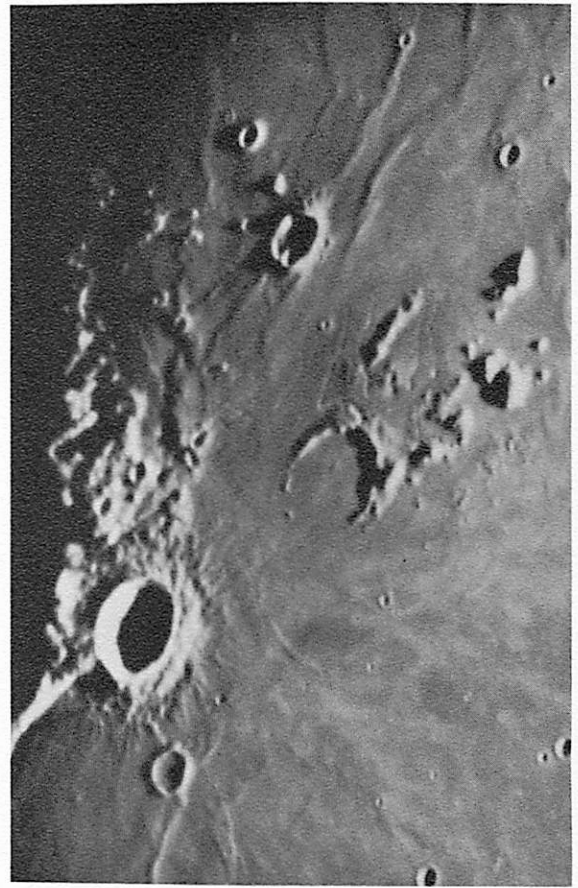
(a)



(b)

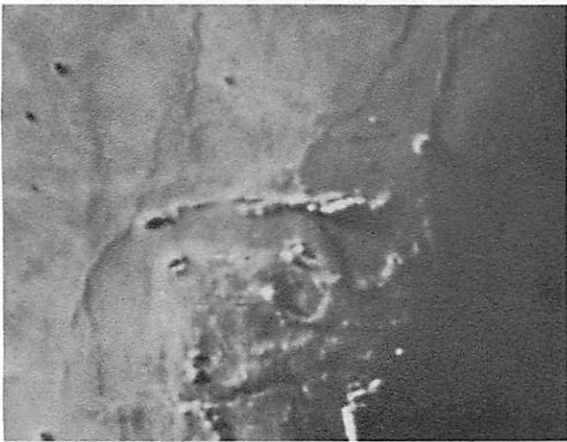


(c)

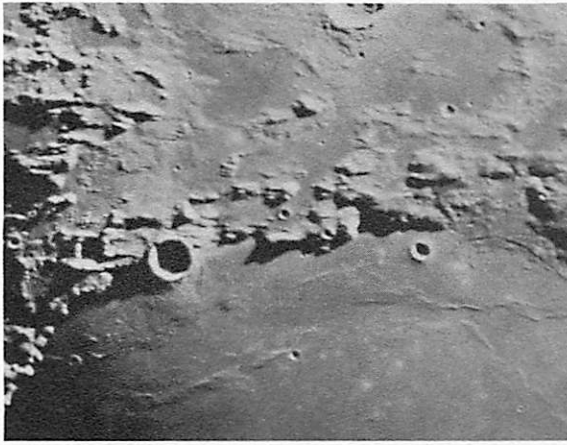


(d)

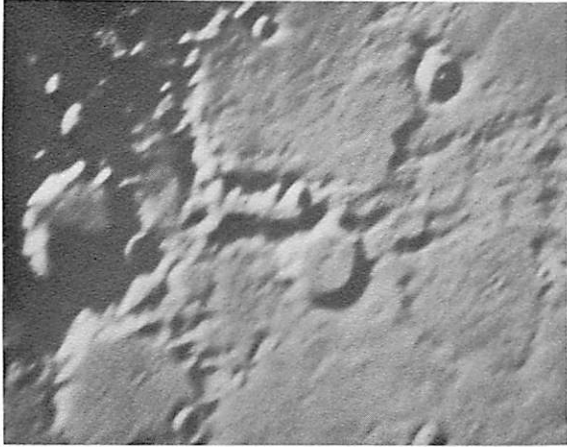
Plate 36.23. Four photographs of radial systems around craters. Note rilles trailing out of small pits in (d). Scale ~ 3 km/mm
(a) Copernicus; McDonald, Mar. 19, 1959; col. 24°0; (b) Eratosthenes; Y1267; col. 13°5; (c) Copernicus; Pic du Midi 37b;
col 22°9; (d) Aristarchus; M624; col. 50°0.



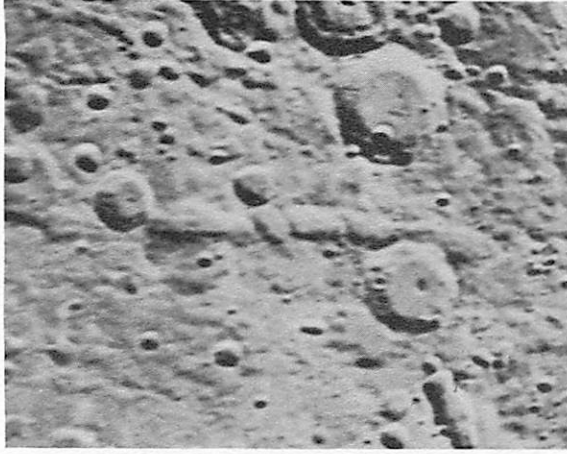
(a)



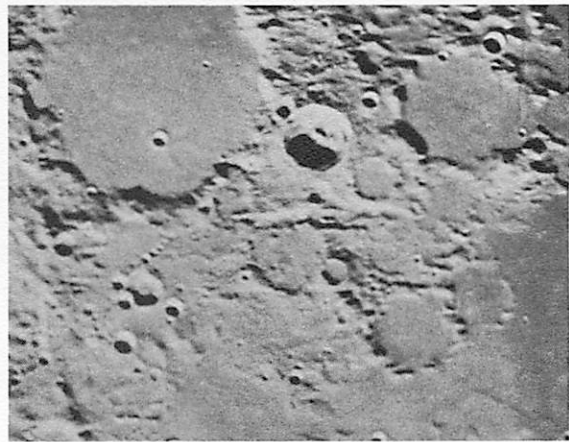
(b)



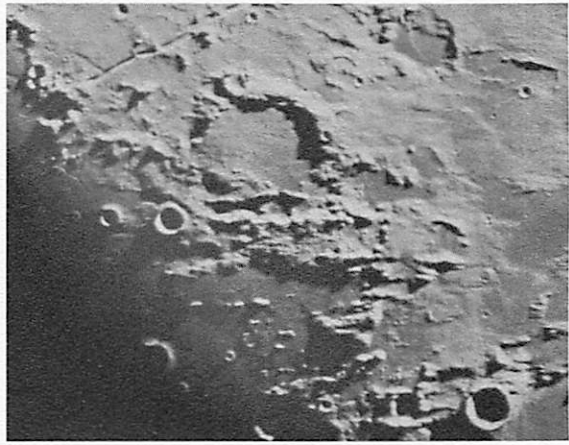
(c)



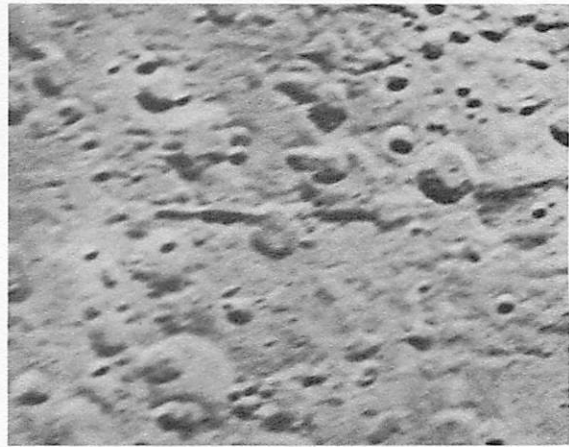
(d)



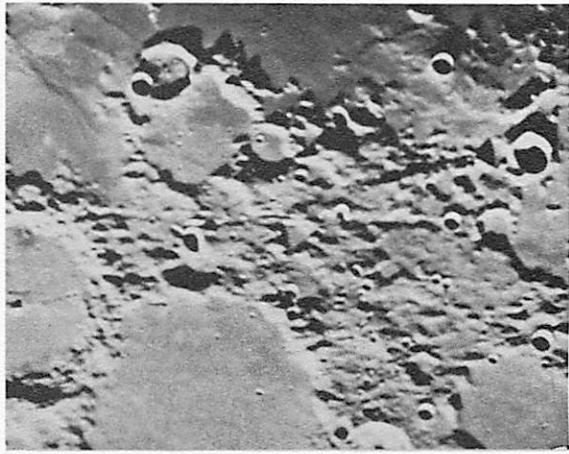
(e)



(f)



(g)



(h)

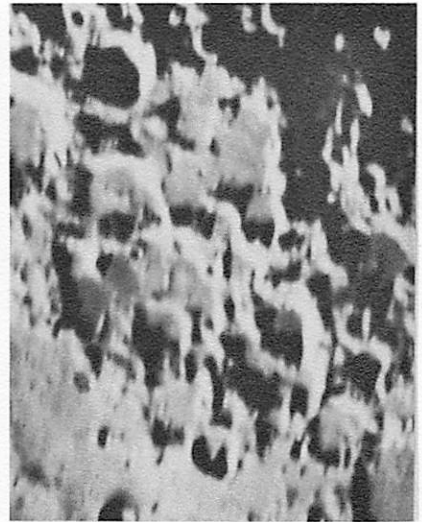
Plate 36.24. Valleys and troughs of radial systems. Direction toward basin is downward. Scale ~ 5 km/mm. (a) Trough on N edge of Aristarchus plateau; Imbrium system; $\sim 34 \times 170$ km; W231; (b) trough in Haemus Mts.; Imbrium system; $\sim 30 \times 110$ km; W111; (c) trough in wall of W. Bondi; $\sim 28 \times 140$ km; Y1350; (d) Rheita Valley; Nectaris system; $\sim 25 \times 330$ km; L193; (e) valley E of Herschel; Imbrium system; $\sim 11 \times 94$ km; Y1261; (f) valley in NE wall of Julius Caesar; Imbrium system; $\sim 17 \times 85$ km; W111; (g) Mallet Valley; Nectaris system; $\sim 12 \times 190$ km; (h) multiple valley W of Ptolemaeus; Imbrium system; $\sim 6 \times 230$ km; Y1261.



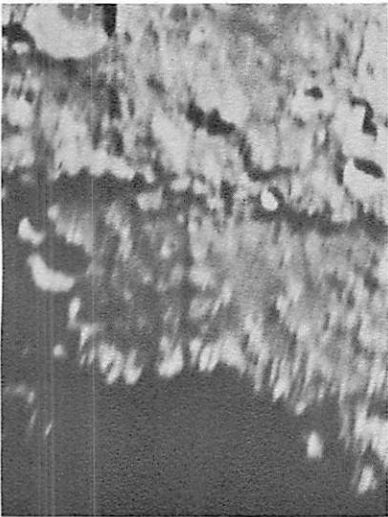
(a)



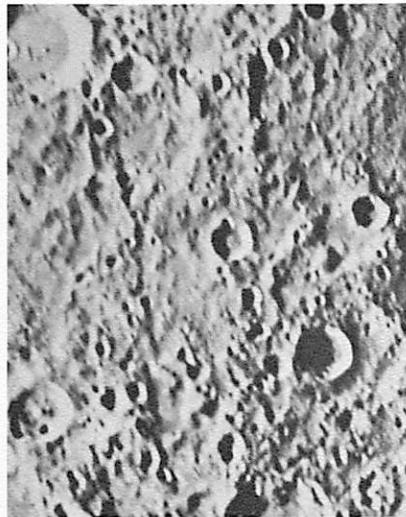
(b)



(c)



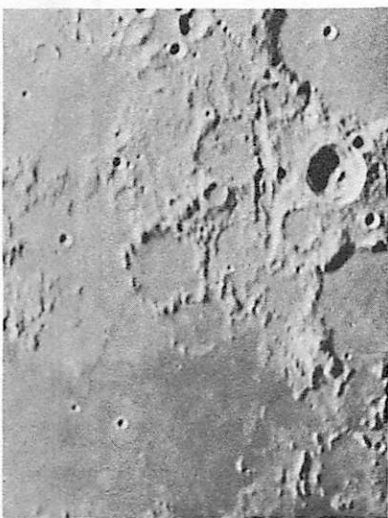
(d)



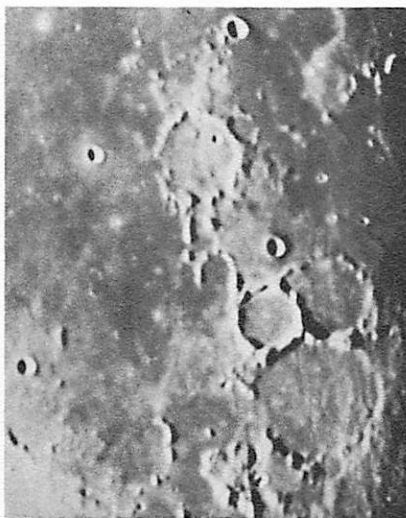
(e)



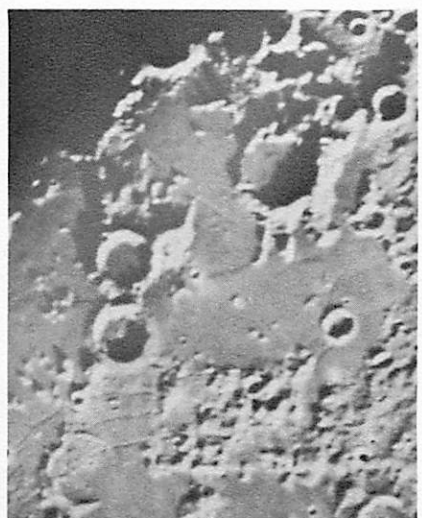
(f)



(g)



(h)



(i)

Plate 36.25. Orthogonal lineaments (*a*, *b*, and *c*), scarps (*d*, *e*, and *f*), deformed craters (*g*, *h*, and *i*) of radial systems. Direction toward basin is downward. Scale ~ 5 km/mm. (*a*) Partial flooding and lineaments near Archimedes; Imbrium system; W115; (*b*) partial flooding and lineaments near Macrobius; Crisium system; L175; (*c*) partial flooding and lineaments near Schickard; Humorum system; W230; (*d*) scarp radial to Humboldtianum; Y482; (*e*) scarps radial to Nectaris; L193; (*f*) scarps radial to Orientale; Y1170; (*g*) Réaumur and Oppolzer; Imbrium lineaments; Y1261; (*h*) Parry M; Imbrium lineaments; Y557; (*i*) Palus Epidemiarum; Humorum lineaments; W171.



Plate 36.26. Full moon with overlay showing the basin systems discussed here. Each line marks a concentric arc or a relatively prominent lineament and each is drawn to proper scale and orientation. Dotted lines give examples of some prominent local grid patterns, not related to basin systems. Not rectified; L224; scale ~ 19 km/mm; col. 82°2.